Translational Oncology 22 (2022) 101450

Contents lists available at ScienceDirect

Translational Oncology

journal homepage: www.elsevier.com/locate/tranon

Advances in PSMA theranostics

Thomas M. Jeitner [a], John W. Babich [a,b,c,1], James M. Kelly [a,c,*]

[a] Molecular Imaging Innovations Institute, Department of Radiology, Weill Cornell Medicine, Belfer Research Building, 413 East 69th Street, Room BB-1604, New York, NY 10021, USA
[b] Weill Cornell Medicine, Sandra and Edward Meyer Cancer Center, New York, NY 10021, USA
[c] Weill Cornell Medicine, Citigroup Biomedical Imaging Center, New York, NY 10021, USA

ARTICLE INFO

Keywords:
PSMA
Theranostics
Targeted radioligand therapy
Targeted alpha therapy

ABSTRACT

The validation of prostate specific membrane antigen (PSMA) as a molecular target in metastatic castration-resistant prostate cancer has stimulated the development of multiple classes of theranostic ligands that specifically target PSMA. Theranostic ligands are used to image disease or selectively deliver cytotoxic radioactivity to cells expressing PSMA according to the radioisotope conjugated to the ligand. PSMA theranostics is a rapidly advancing field that is now integrating into clinical management of prostate cancer patients. In this review we summarize published research describing the biological role(s) and activity of PSMA, highlight the most clinically advanced PSMA targeting molecules and biomacromolecules, and identify next generation PSMA ligands that aim to further improve treatment efficacy. The goal of this review is to provide a comprehensive assessment of the current state-of-play and a roadmap to achieving further advances in PSMA theranostics.

Introduction

Prostate specific membrane antigen (PSMA) is highly and selectively expressed on prostate cancer cells. Consequently, there is significant interest in ligands that bind PSMA as a means of visualizing and treating these cancers. Despite the interest in PSMA, its functions in normal or neoplastic prostate cells are poorly understood. Understanding the biology of this protein may inform efforts to better target PSMA and the associated cancers, just as the use of PSMA ligands has already indicated new aspects of prostate cancers and its treatment. Here, we provide a brief review of the biology of PSMA, as well as an overview of ongoing efforts to develop PSMA ligands as theranostic (diagnostic + therapeutic) agents.

Part 1: the biology and biochemistry of PSMA

PSMA: gene and proteins

PSMA is known by several names - glutamate carboxypeptidase II (GCPII), *N*-acetylated-α-linked acidic dipeptidase [1,2], and folate hydrolase (FOLH1) [3,4] - which reflect the activities of this enzyme in different tissues. These proteins are actively transcribed from one of two copies of the *FOLH1* gene. The relevant gene is situated at position 11.12 on the p arm of chromosome 11 (GenBank: AF007544) [5,6], while a pseudogene is located on the other arm at position 11.14 [7]. A total of 19 exons and 18 introns [5,6] comprise the gene, which also contains multiple start sites that give rise to distinct products at different sites [2,8–13]. Of these products, PSMA and FOLH1 are 100% homologous [10] while PSMA/FOLH1 and GCPII are 83% homologous [14–16]. Normal prostate cells express an FOLH1 transcript that encodes a cytoplasmic protein of unknown function [9,11,17,18]. By contrast, cancerous prostate cells produce full-length PSMA [19]. The expression of this protein increases as a function of cancer progression [20], Gleason score, and serum PSA levels [21]. PSMA expression, however, is not restricted to prostate cancer. Endothelial cells from virtually all other cancers also express PSMA [19,22–31]. In addition, normal tissues, such as the small intestine, kidney nephron, brain, and salivary glands, express PSMA [4,16,32–36].

Although a promoter for FOLH1 exists [6], the prostate-specific expression of PSMA is primarily controlled by a *cis* acting element known as the PSMA enhancer or *PSME* [37]. Binding of NFATc1 to AP-3

Note: We do not feel that a graphical abstract is required for this review article, but submit the following for consideration.

* Corresponding author at: Department of Radiology, Weill Cornell Medicine, Molecular Imaging Innovations Institute, Belfer Research Building, 413 East 69th Street, Room BB-1604, New York, NY 10021, USA.
E-mail address: jak2046@med.cornell.edu (J.M. Kelly).
[1] Present address: Ratio Therapeutics, Inc, Boston, MA, USA.

https://doi.org/10.1016/j.tranon.2022.101450
Received 7 March 2022; Received in revised form 4 May 2022; Accepted 8 May 2022

site in the 5′ end of *PSME* facilitates PSMA expression [38], whereas binding Sox7 to a number of sites within *PSME* suppress its expression [39,40]. Sox7 is frequently inactivated in prostate cancer by promoter hyper-methylation, in agreement with the enhanced expression of PSMA in some forms of this cancer [41]. *PSME* driven expression is also repressed by androgens consistent with its role in prostate biology and carcinogenesis [37].

FOLH1 encodes a 750-residue membrane-associated, dinuclear zinc peptidase with an apparent molecular mass of 110 kDa [42]. Glycosylation accounts for the disparity between the predicted and apparent mass. The bulk of this enzyme is resides on the outer surface of the plasma membrane tethered by a membrane-spanning segment of 22 amino acids. An additional 19 residues project into the cytoplasm. The extracellular portion folds into three domains, the protease, apical and C-terminal domains [43]. FOLH1 dimerizes to form the active enzyme with the C-terminus of one monomer interfacing with the protease and apical regions of the other monomer. The enzymes encoded by *FOLH1* catalyze the hydrolysis of terminal glutaminyl residues from substates bearing glutaminyl (*N*-acetyl aspartylglutamate: NAAG) or polyglutaminyl residues (folates). Substrates bind to the enzyme by way of a hairpin formed from a β sheet in the C-terminal domain. The hairpin situates specific lysyl (K699) and tyrosyl (Y700) residues in close proximity the carboxyl moieties of the glutamate portion of the substrate and effectively sense the glutarate portion of the substrate (Fig. 1). This sensing involves the ε-amino group of the lysyl residue forming a salt bridge with the γ-carboxyl group and the hydroxyl group of the tyrosyl residue to form a hydrogen bond with the α-carboxyl group of the glutaratic moiety. Binding of the substrate induces conformational changes that position the amide of the glutamyl substrate so that it hydrogen-bonds with the γ-carboxyl group of a glutamyl residue (E424) in the active site, causing the now basic active-site glutamate to abstract a proton from a water molecule ligated by two zinc atoms. The resulting hydroxyl ion then attacks the proffered peptide bond of the bound substrate. Following hydrolysis, the catalytic glutamyl residue shuttles the proton to the amino group of the leaving product.

GCPII and the regulation of extrasynaptic glutamate and NAAG pools

Arguably, some of the most exciting and informative recent work on PSMA comes from studies of GCPII in the brain, where it contributes to several major pathologies. GCPII (EC 3.4.17.21) acts to catabolize extrasynaptic NAAG in the brain [16,32,44]. NAAG is the most abundant peptide neurotransmitter present in the brain, as well as the third most prevalent neurotransmitter overall [45,46]. These rankings equate to millimolar amounts of NAAG in the brain. Consequently, hydrolysis of NAAG by GCPII yields millimolar quantities of glutamate. Additional amounts of glutamate are also released from the same neurons that release NAAG [45] and through the actions of another NAAG peptidase termed glutamate carboxypeptidase III (EC 3.4.17.11) [47,48]. Glutamate is the most potent excitatory neurotransmitter in the brain and excess levels elicit lethal accumulations of intraneuronal calcium following its engagement with post-synaptic *N*-methyl-D-aspartate (NMDA) receptors [49]. NAAG is also an NMDA antagonist [50]. Thus, its catabolism will augment signaling via NMDA receptors. Astrocytes and other glial cells protect the brain from excitotoxicity by scavenging glutamate. The scavenged glutamate is then converted to either 2-oxoglutarate (α-ketoglutarate) for anaplerosis, or to glutamine for export to the neighboring neuron [51]. However, pathological conditions result in the accumulation of NAAG to such high levels that the resulting amounts of glutamate exceed the capacity of neighboring glia to effectively scavenge it. The ensuring excitotoxicity contributes to neurodegeneration. GCPII inhibitors, therefore, hold great promise in the treatment of neurodegenerative diseases like Alzheimer Disease and amyotrophic lateral sclerosis [46,52]. Many of these inhibitors also form

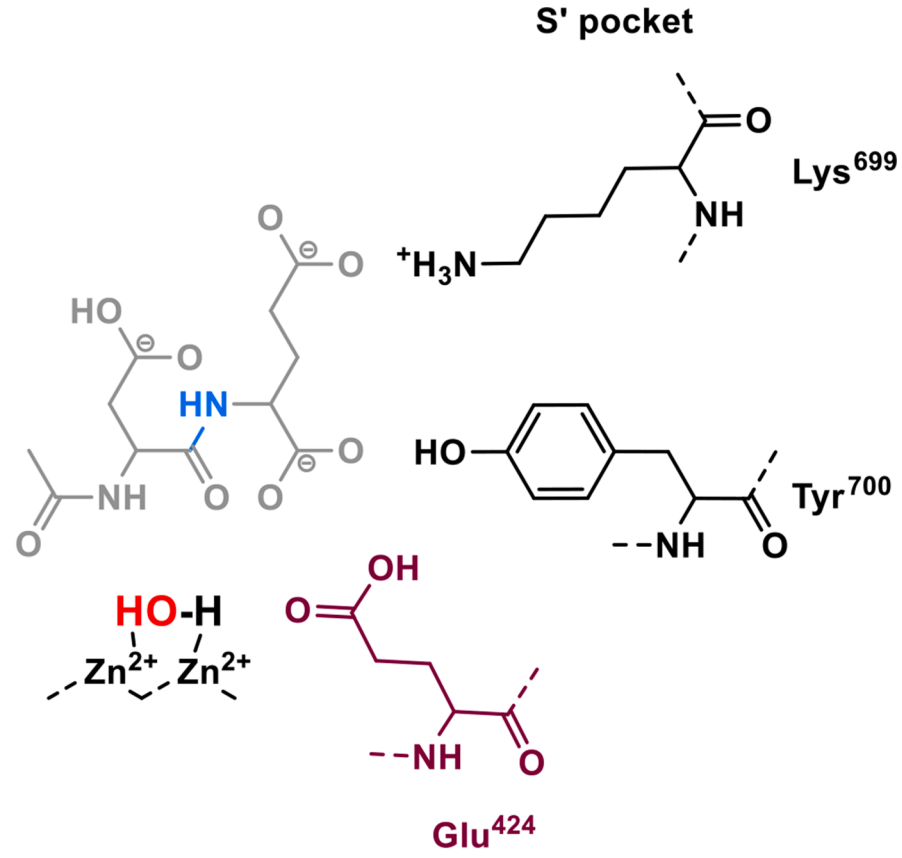

Fig. 1. Glutarate Sensing in the Glutamate Carboxypeptidase Active Site
The major glutarate sensing residues - Lys699 and Tyr700 - of the S' binding pocket are shown in black. These residues interact with the α and γ carboxyl groups that define the glutarate portion of N-acetyl aspartylglutamate (gray). Binding of the substrate to the S' pocket causes the amide (blue) of glutamyl substrate to hydrogen bond with γ-carboxyl group of Glu424 (magenta) inducing it to abstract a proton from the water molecule ligated by the zinc atoms. The resulting hydroxyl ion (red) then attacks on the neighboring peptide bond (blue). Following hydrolysis, the catalytic glutamyl residue shuttles the proton to the amino group of the leaving product. For the sake of clarity, a number of interactions are not included (for full details see Mesters et al., [43]).

the basis of theranostics that target PSMA [53].

NAAG perpetrates its actions as a neurotransmitter by binding metabotropic glutamate receptor 3 (mGluR3), which is situated postsynaptically in the higher cortical circuits of primates [54]. Activation of these receptors strengthens synaptic connectivity. Conversely, decreasing amounts of NAAG correlate with decreases in cognition [54,55]. These decreases in NAAG, in turn, correlate with increased amounts of GCPII due enhanced transcription of a FOLH1 missense polymorphism (rs202676) [56] or cerebral inflammation [57]. The FOLH1 missense mutation (rs202676 G allele) is associated with increased levels of FOLH1 mRNA in the dorsolateral prefrontal cortex of the human brain. This increase in message is likely to be translated into GCPII given the decreased amount of NAAG measured in the centrum semiovale [56]. GCPII is expressed in astrocytes, microglia, neuropil, and neurons [33,57–61]. Of these cells, astrocytes and microglia mediate the inflammatory response in the brain, and during inflammation these cells express elevated levels of GCPII [57,60–62]. Datta et al. postulate that inflammation may also cause neurons to endocytose GCPII uptake based on neuronal GCPII staining in aging neurons [57] and neurons exposed to hypoxia or ischemia [60]. These cell specific increases in GCPII are evident in advanced aging [57] and multiple sclerosis [52], both of which are associated with cognitive dysfunction [63,64]. Importantly, GCPII inhibition improves cognition in animal models of aging [57] and multiple sclerosis [52,55], as well as cerebral inflammation [65] and cognitively intact animals [54]. The use of GCPII inhibitors in the brain and periphery was recently reviewed elsewhere [53].

Despite the clear relationship between inflammation and GCPII expression, the role of inflammatory mediators – reactive oxygen species, reactive nitrogen species, or cytokines – in regulating this expression is poorly understood. Although lipopolysaccharide is not a cytokine, it causes cells to produce and release cytokines, and its addition to primary microglia markedly increases GCPII activity in these cells [60]. Similarly, CXCL1 significantly increased in the cortex of superoxide dismutase transgenic mice subjected neonatal hypoxic-ischemic brain injury [61]. Prior administration of a GCPII inhibitor to these mice mitigated the increase in CXCL1. Given the interplay of pro- and anti-inflammatory cytokines, more detailed studies of the role of these and other inflammatory mediators in GCPII expression is likely to yield more candidates for the regulation of this activity in physiological and pathological states.

Intestinal PSMA or folate hydrolase 1 and folate metabolism

The intestinal form of PSMA is situated on the jejunal brush border membrane where it converts dietary folates into a form capable of absorption by the small intestine [4] (Fig. 2). Folates encompass a series of compounds that contain a pteroic acid moiety bound to a single glutamate (folinic acid, 5-methyltetrahydrofolate, and folic acid) or a chain of γ-linked glutamates (polyglutamyl folinic acids) [66]. Mammals cannot synthesize folate and must consume foods rich in these compounds – typically legumes – to obtain tetrahydrofolate, a crucial vitamin coenzyme for one-carbon metabolism. Put simply, one carbon metabolism refers to reactions involving methyl, methylene, and formyl group transfers. These groups are highly reactive and are therefore bound to carriers, such as tetrahydrofolate to facilitate their participation in metabolic processes. A common example of these reactions is the formation of 10-formyltetrahydrofolate or formyl folate, which is required for the biosynthesis of inosine monophosphate. The latter molecule is the precursor to GMP and AMP, which following modification to the

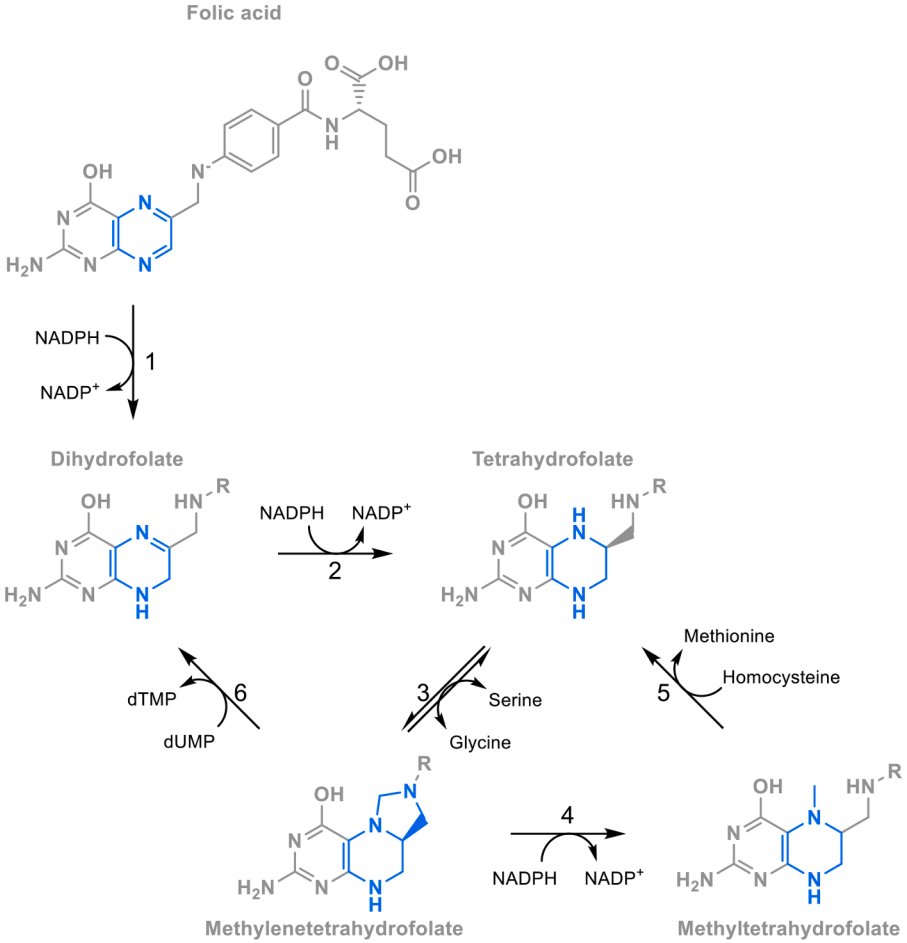

Fig. 2. Folic Acid Metabolism
Reactions 1 and 2 are catalyzed by dihydrofolate reductase (EC 1.5.1.3): folic acid is reduced to dihydrofolate, which in turn is reduced to tetrahydrofolate. Serine hydroxymethyltransferase (EC 2.1.2.1) catalyzes *reaction 3*. The reaction product, N^5N^{10}-methylene tetrahydrofolate, can then be reduced to N^5-methyl tetrahydrofolate by methylenetetrahydrofolate reductase (EC 1.5.1.20), as shown in *reaction 4*. Methyltetrahydrofolate, in turn, is the methyl donor for the methylation of homocysteine to form methionine, as catalyzed by homocysteine methyltransferase (EC 2.1.1.10, *reaction 5*). This reaction also regenerates tetrahydofolate. Dihydrofolate is also regenerated through the actions of thymidylate synthase (EC 2.1.1.45, *reaction 6*), which catalyzes the reductive methylation of deoxyuridine monophosphate (dUMP) to form deoxythymidine monophosphate (dTMP). In this reaction, methyltetrahydrofolate is oxidized to dihydrofolate. dTMP is the source of the thymidine used to synthesized DNA. Note, the majority of the indicated changes affect the pteroyl portion of the folates and these are indicated in blue.

sugar backbone, gives rise to the nucleotides for nucleic acid synthesis. Dietary folate exists primarily with chains of greater than two glutamyl residues, e.g., pteroylhexaglutamate [66]. Intestinal absorption requires that γ-linked glutamates be removed from the polyglutamyl folates. In the case of polyglutamyl folinic acid, this means conversion to folinic acid, and folate hydrolase 1 catalyzes the hydrolysis of γ-linked glutamyl moieties from polyglutamyl folates [4]. The contention that the enzyme favors the polyglutamyl folates is supported by the observation that polyglutamyl folinic acid binds to the catalytic site more efficiently than does folinic acid or its metabolite, 5-methyltetrahydrofolate (Fig. 2). The absorbed pteroyldiglutamate then collects in the hepatic vein for transport to the liver for reduction to methyltetrahydrofolate: the major circulating form of folate [67,68].

Renal PSMA

A diverse range of ligands cause PSMA to endocytose. These ligands range in size from antibodies to molecules with the dimensions of small peptides [69–72]. Neither the rates of PSMA internalization nor of recycling to plasmalemma are known. Even so, the endocytosis and recycling of PSMA are thought to be similar that of the transferrin receptor given the characteristic of their leucine zipper domains as well as other structural and sequence similarities [6,73]. Endocytosed PSMA and the transferrin receptor also appear in the same vacuoles [74]. The rates of transferrin receptor recycling should therefore approximate those of PSMA. The transferrin receptor recycles at a rate of 0.63 min^{-1} [75], which implies that PSMA should recycle to plasmalemma within 2 min of internalization. The rate of this recycling decreases as a function of receptor number and as the size of the ligands increase [75,76]. If this proves true for PSMA as well, small molecules should induce PSMA to endocytose more rapidly than do antibodies.

Renal and prostatic PSMA are thought to act as a ancillary folate transporters, such that in the absence of cleavable substrate, pteroyldiglutamates cause PSMA to endocytose and deliver its cargo to cells [77]. This argument is based on the following observations: in the kidney, circulating folates are re-absorbed via renal tubular absorption from the blood by folate receptor alpha (FRα), and loss of this receptor significantly attenuates, but does not completely prevent folate re-uptake by the kidneys [78]. The continued uptake of folate in FRα-deficient animals implies the existence of another route for renal folate transport. One candidate for this transport is PSMA, which is also expressed in regions responsible for renal folate uptake [79]. Folic acid inhibits the folate hydrolase activity of PSMA, which implies that it binds PSMA at least transiently [77,80]. PSMA also enables folic acid

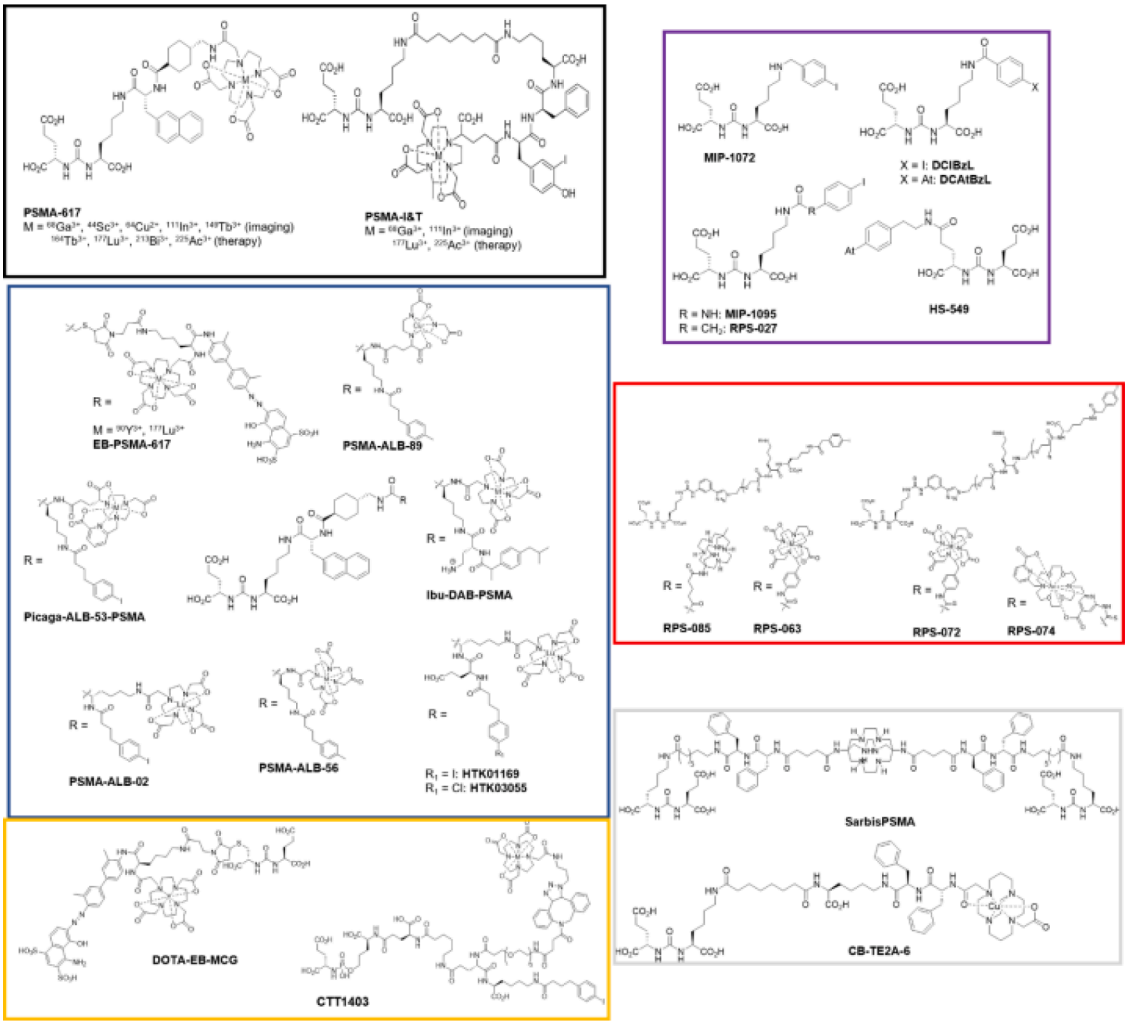

Fig. 3. The structures of small molecule PSMA theranostic ligands discussed in this manuscript. The library is not exhaustive, but reflects the different classes of molecule currently under investigation. The compounds highlighted in the black square (PSMA-617 and PSMA-I&T) have undergone the most extensive clinical evaluation to date and are templates for next generation ligands. The compounds highlighted in the purple square are radiohalogenated PSMA inhibitors. Compounds in the blue box are albumin binding ligands based on PSMA-617, while the compounds in the red and orange boxes are albumin-binding ligands based on other platforms. Finally, the molecules in the gray box are PSMA ligands designed for $^{64/67}$Cu theranostics.

uptake by cells that express it [77]. Endocytosis and subsequent dissociation of the PSMA and folic acid is therefore the most likely mechanism for the ingress of folic acid. This hypothesis is supported heuristically by the observations that PSMA polymorphisms that decrease its enzymatic activity increase serum folate concentration in kidney transplant patients [81], as well as the renal uptake of highly selective ligands for PSMA [82–88].

The identities of the natural ligands for renal PSMA are not known. Since the circulating folates are all monoglutamylated and therefore not subject to hydrolysis by glutamate carboxypeptidases, the binding of folate analogs to renal PSMA may serve as a mechanism for either recovery into the folate pool – as in the case of folic acid – or the elimination of the analogs. In other words, prolonged or high affinity occupancy of the PSMA folate binding site by folate analogs may promote endocytosis and the subsequent metabolism of the analogs. Folic acid can be reduced to methyltetrahydrofolate by dihydrofolate reductase and utilized in one-carbon metabolism (Fig. 2).

Salivary gland PSMA

Hominin salivary glands express low levels of PSMA [36,89–91]; moreover, this expression is restricted to specific sites, such as the intercalated ducts of submandibular glands [36]. This specificity presumably accounts of the equivocal reports of PSMA staining in these glands [19,36,89–91]. Despite the low expression of PSMA, salivary glands sequester PSMA ligands [36,82,92–95]. Given the discordance between PSMA expression and PSMA ligand sequestration by the salivary glands, Rupp et al. [36] hypothesize that an entity other than PSMA is responsible for the uptake of its ligands but do not suggest an alternate uptake mechanism for the PSMA ligands. This conclusion is supported by recent data confirming that only some of the binding to salivary glands can be displaced by non-radioactive PSMA ligands, with a substantial fraction of the uptake appearing to be non-specific [96]. This is an important issue, because the salivary uptake of these ligands is the major impediment to the use of these agents as a means of delivering therapeutic doses of radiation to prostate cancer [93–95,97–99].

Prostate PSMA as a putative glutamate carboxypeptidase

Prostatic PSMA catalyzes the hydrolysis of γ-linked glutamate from polyglutamyl folates [80]. The relevant substrates for this reaction, however, are not present in the circulation. O'Keefe et al. [100] proposed that these substrates may be derived from cells dying within the tumor mass. Tetrahydrofolate can be converted to polyglutamyl folate by way of folylpoly-γ-glutamate synthetase, and cells do contain polyglutamyl folate stores [101–103]. The liver contains the highest amount of polyglutamyl folate equal to 14 nmole per gram of rat tissue, equivalent to 12 μM polyglutamyl folate [103]. Just as in normal tissues, tumor masses exhibit ongoing cell death, albeit at a slower rate than that of cell proliferation. Again, just as in normal tissues, phagocytes consume dying cells in tumors. Cell lysis leading to the spillage of polyglutamyl folates is therefore an unlikely event in cancers. Notably, O'Keefe et al. [100] did not provide any measurements of polyglutamyl folate release from tumors to support their hypothesis.

Prostatic PSMA is also proposed to act as a carboxypeptidase to cleave circulating pteroyldiglutamate to release glutamate to activate metabotropic glutamate receptors [104]. This proposal is based, in part, on the well-known hydrolysis of NAAG by GCPII to yield glutamate. In both cases, α-linked glutamate is released from either pteroyldiglutamate or NAAG. However, no *direct* measurements of this release from pteroyldiglutamate as catalyzed by PSMA exist. Instead, Kaittanis et al. [104] reported an *indirect* measurement of glutamate, namely an increase in glutamate-induced fluorescence following incubation of PSMA-bearing cells with pteroyldiglutamate. At the time of the incubation, the cells were starved of both pteroyldiglutamate and glutamate. Thus, pteroyldiglutamate was added to metabolically stressed cells under non-physiological conditions that could have promoted glutamine catabolism to supply glutamate. In other words, the glutamate-induced fluorescence could have been due to metabolic changes rather than to the activity of PSMA *per se*. In any case, the other major difficulty with this proposal is that serum levels of glutamate far exceed those of pteroyldiglutamate. Serum contains 51 μM glutamate [103] and between 20 and 60 nM pteroyldiglutamates, depending on age [67,68]. Thus, even if PSMA were to cleave glutamate from pteroyldiglutamate, the amounts released would be a thousand-fold lower than the amounts of glutamate already present in blood. Kaittanis et al. [104] also base their arguments on the apparent activation of signaling pathways by glutamate interacting with metabotropic glutamate receptors without considering that the same pathways are activated by endocytosis 105–108] that could also account for importation of folates.

While the above discussion argues against PSMA acting as a glutamate carboxypeptidase in prostate cancer, the truncated form of PSMA found in normal prostate tissues may be a γ-glutamyl hydrolase [109]. The latter protein shares the active site but not the cytoplasmic tail or transmembrane portions of the full length PSMA [11,18]. Thus, the truncated PSMA that is constrained to the cytoplasm may act to remove the glutamyl chains from the intracellular polyglutamyl folates when necessary.

Prostate PSMA as a pteroyldiglutamate transporter

Based on the above considerations and those that follow, we hypothesize that PSMA is expressed in prostate cancer for the importation of pteroyldiglutamate by clathrin-mediated endocytosis. This hypothesis is based, in part, on the established relationship between blood folate levels and the degree of prostate cancer aggressiveness [110]. Interestingly, the amount of circulating total folate increases with age in adults, as does the risk of prostate cancer [67,68,111]. In their first ten years, US males average 52 nM of total serum folate that subsequently falls to a nadir of 28 nM during their twenties and then rises linearly to a value of 55 nM for men in their eighth decade [111]. The slope of this linear increase as a function of dietary folate intake; the serum of men in their eighties consuming over 1000 μg folate per day contains an average 89 nM folate [111]. In the US, cereal grains are fortified with synthetic folic acid to mitigate the incidence of neural tube defects [112–114]. Dihydrofolate reductase catalyzes the reduction of folic acid to tetrahydrofolate. The activity of this enzyme is low in most tissues, including liver, and limits the metabolism of folic acid. Consequently, unmetabolized folic acid arises in blood when the amounts of ingested folic acid exceed 400 μg [115,116]. This overdosing is compounded in humans, which in addition to having less than 2% of the hepatic dihydrofolate reductase activity of rats, exhibit a five-fold variation in this activity [117]. Therefore, one unintended effect of folic acid fortification is the evolution of metabolized folic acid in the blood [68,118,119]. The amounts of metabolized folic acid parallel the aforementioned trends in total blood folate [111] and constitute approximately 4% of the total serum folate from 1 to 60 years of age [68]. At later ages, the unmetabolized folic concentrations can reach 13 nM equaling 10% of the serum total folate [68]. Obeid et al. [120] also reported that dosing elderly subjects with folic acid for 3 weeks increased serum folate levels from 0.08 to 15.5 nM (the subjects are German and therefore were not subjected to mandatory folic acid supplementation, hence the lower baseline levels than those reported for the US population [111] and cited above).

Folic acid is reduced by dihydrofolate reductase to tetrahydrofolate which forms a complex with thymidylate synthase to channel substrates for DNA synthesis [121]. The thymidylate synthase reaction produces dihydrofolate, a very potent inhibitor of methylene tetrahydrofolate reductase which shunts the folate pathway toward methionine biosynthesis and away from DNA metabolism. Dihydrofolate formation assures that the folate analogues are used for DNA synthesis. The diseased prostate contains high levels of dihydrofolate reductase activity [122].

Prostate cancer cells should thus have a growth advantage in the presence of a ready supply of folic acid and a means to import this folate. As noted earlier, the blood of older US males contains significant amounts of unmetabolized folic acid and other folates. The expression of PSMA in these men could therefore serve to import folic acid into the prostate and thereby promote DNA synthesis and anaplerosis in the resident neoplastic cells. In support of this hypothesis, PSMA facilitates folic acid uptake by neoplastic prostate cells induced to express PSMA [77]. Folic acid also blocks the uptake of the major circulating folate, methyltetrahydrofolate, by PSMA [123]. Thus, cells expressing both high levels of PSMA and dihydrofolate reductase may preferentially metabolize folic acid to support DNA synthesis (Fig. 2, reactions 1–3 and 6) rather than other aspects of one-carbon metabolism, as would be expected with methyltetrahydrofolate (Fig. 2, reaction 6).

Prostate PSMA in cancer

We hypothesize that PSMA plays an important role in glutamate and folate metabolism, but its function remains poorly understood. Notwithstanding its specific contributions to tumor development and progression, PSMA is an outstanding target for theranostic radiopharmaceuticals. In addition to its elevated expression in prostate cancer cells, PSMA is a type II transmembrane protein with glutamate-carboxypeptidase activity and a known substrate. Furthermore, upon ligand binding, PSMA is internalized via clathrin-coated pits and subsequent endocytosis, resulting in an effective transportation of the bound molecule into the cells. Since internalization leads to enhanced tumor uptake and retention, targeting PSMA is expected to result in high image quality and high doses of cytotoxic radiation absorbed by tumor cells. In Part 2 of this review, we summarize PSMA theranostic ligands in development and in clinical use.

Part 2: PSMA theranostic ligands

The concept of theranostics arose out of the potential to combine diagnostic and therapeutic capabilities in a single ligand. However, as the ideal pharmacokinetics for diagnostic applications (rapid accumulation in tumors, rapid clearance from non-target tissue, and no requirement for prolonged tumor retention) and therapeutic applications (high tumor uptake and prolonged retention and a biological half-life that is well-matched to physical half-life) differ, there has recently been a shift towards the use of one PSMA-targeting ligand for diagnosis and a separate ligand for evaluating tissue distribution, predicting dosimetry, and delivering therapeutic ionizing radiation. This review chooses to highlight PSMA-targeting ligands of the latter category due to their potential application in personalized medicine. However, we wish to highlight the fact that numerous PSMA-targeting ligands used exclusively for diagnostic purposes are under development. These are typically small molecule ligands with rapid tissue distribution and are reviewed elsewhere [124–128]. ^{68}Ga-PSMA-11 [129] and ^{18}F-DCFPyL [130] recently received FDA approval and are marketed as Ga68 PSMA-11 and Pylarify®, respectively. Both ^{68}Ga-PSMA-11 and ^{18}F-DCFPyL are cleared renally, leading to high bladder accumulation. As this can be disadvantageous for imaging metastases proximal to the prostate gland [131], new alternatives with more favorable clearance profiles are in various stages of clinical evaluation, including ^{18}F-PSMA-1007 [132,133], ^{18}F-CTT1057 [131], and ^{18}F-JK-PSMA-7 [134,135]. Numerous single photon computed tomography (SPECT) agents for detecting prostate cancer by planar imaging have been developed in parallel to these PET agents. Among the SPECT agents to undergo preliminary clinical evaluation are ^{99m}Tc-MIP-1404 [83], ^{99m}Tc-MIP-1427 [136], ^{99m}Tc-PSMA-T4 [137], ^{99m}Tc-PSMA-I&S [138] and ^{99m}Tc-EDDA/HYNIC-iPSMA [139]. As an alternative strategy, radiohybrid PSMA ligands incorporating fluorine-18/fluorine-19 and macrocyclic radiometal chelators have been developed as theranostic agents that exploit the superior imaging properties of fluorine-18 [140]. Among this new class of compounds, ^{18}F-rhPSMA-7.3 has undergone preliminary clinical evaluation and is under FDA review [141].

Clinically advanced theranostic PSMA ligands

The first generation of PSMA-targeting agents were antibodies conjugated to radiometals for imaging or therapy. The ^{111}In-labeled monoclonal antibody 7E11-C5.3 [142] (marketed as ProstaScint®) provided early validation of this PSMA targeted theranostic approach in advanced prostate cancer. Nevertheless, despite uptake in primary disease and metastatic lesions [142], 7E11-C5.3 targets an intracellular epitope on PSMA [89], restricting its ability to bind viable cells. Subsequent development of J591, a humanized monoclonal antibody against the external domain of PSMA, stimulated renewed clinical investigation into PSMA-targeted imaging and therapy of progressive disease [143]. J591 has undergone evaluation in men with metastatic castration-resistant prostate cancer (mCRPC) as an ^{111}In-DOTA conjugate for SPECT imaging [144], an ^{89}Zr-DFO conjugate for PET imaging [145], ^{90}Y- [146] and ^{177}Lu-DOTA [147] conjugates for targeted b-particle therapy, and an ^{225}Ac-DOTA conjugate for targeted α-particle therapy [148]. Phase II clinical trials with ^{177}Lu-J591 have been completed, in which the response rate in treated patients, defined as $\geq$ 50% decrease in PSA, is 11% [147]. As a result of a circulation half-life in excess of 1 day [144], hematological toxicity is dose limiting [146]. Ongoing Phase I clinical trials with ^{225}Ac-J591 highlight response even in patients with prior ^{177}Lu-J591 PSMA-targeted radiotherapy, with no non-hematological grade 3/4 adverse events [149].

Small molecule alternatives to J591 have proliferated following the identification of a high affinity heterodimeric urea pharmacophore for PSMA binding [150]. The chemical structures of leading examples of small molecule PSMA inhibitors are depicted in Fig. 3. In comparison to monoclonal antibodies, small molecules are excreted more rapidly, thereby reducing the likelihood of hematological toxicity. The majority of ligands to reach clinical trials incorporate a glutamate-urea-lysine (EuK) moiety for PSMA targeting. The first potential PSMA theranostic ligands were high-affinity small-molecule inhibitors of PSMA containing radioiodine, ^{123}I-MIP-1072 and ^{123}I-MIP-1095 [151]. The iodophenylurea derivative of EuK, MIP-1095, is a true theranostic ligand that shows clear delineation of tumor lesions when labeled with the positron-emitting radioisotope ^{124}I and induces reductions in PSA, pain, and tumor volume in most patients when labeled with the β-emitting radioisotope ^{131}I [82]. The response rate reaches 70% following a single cycle of ^{131}I-MIP-1095 therapy, although relapse is typical. Subsequent cycles do not appear to improve response, while xerostomia and hematological toxicities increase [93]. Xerostomia arises from physiologic uptake of the radioligand in the parotid and other salivary glands [82]. By contrast, hematological toxicities are likely due to the high energy β-particles ($E_{\beta(max)}$ = 606 keV) emitted from ^{131}I-MIP-1095 that accumulates in bone metastases. These particles travel a mean distance of 2.4 mm, which may allow escape from bone lesions into the neighboring marrow.

In comparison to ^{131}I, ^{177}Lu emits lower energy β-particles ($E_{\beta(max)}$ = 497 keV) that travel a mean distance of 0.7 mm in soft tissue. Theranostic PSMA-targeting ligands bearing a macrocyclic chelator for complexation of $^{177}Lu^{3+}$ enable the favorable physical properties of this radionuclide to be harnessed for targeted radioligand therapy. The most widely studied ligand of this class, PSMA-617, incorporates a DOTA moiety for chelation of trivalent radiometals including $^{68}Ga^{3+}$ [152, 153] and $^{177}Lu^{3+}$ [86]. In agreement with MIP-1095, ^{177}Lu-PSMA-617 exhibits physiologic uptake in salivary and lacrimal glands, and kidneys. The dose to these structures is up to 10 times lower than that for ^{131}I-MIP-1095 [154]. The efficacy of ^{177}Lu-PSMA-617, now marketed as Pluvicto®, has been evaluated in multiple clinical centers across the world [99,155–160] and received NDA approval from the FDA in March 2022 for the treatment of men with mCRPC upon conclusion of the phase III VISION clinical trial [160]. The characteristics of the patients

included in these studies vary and are reviewed elsewhere [161]. These studies report a response rate of 45–55% following multiple cycles of ^{177}Lu-PSMA-617 [161,162], with median overall survival of 14 months [99,162] and progression-free survival of 8 months [162]. Mild or transient xerostomia was reported in approximately 10% of patients [98], and increased at higher doses [162]. This toxicity became dose-limiting in patients undergoing targeted alpha therapy (TAT) with ^{225}Ac-PSMA-617 [94,163]. Notwithstanding elevated toxicity in salivary and parotid glands, the response rate of patients undergoing single dose TAT exceeds 60% [163,164], with the majority of these patients experiencing a PSA decline > 80%, and responses are observed even in patients who are refractory to β-particle therapy [94] or who have brain metastases [165]. Dose de-escalation appears to reduce xerostomia in some patients without compromising therapeutic efficacy [164]. The average progression-free survival is 9 months, which compares favorably to treatment of earlier stage disease [163].

A second EuK-based PSMA ligand, known as PSMA-I&T, bearing a DOTAGA chelator has undergone preliminary investigation in multiple centers. In one cohort of patients, a response rate of 60% was observed following up to 5 cycles of ^{177}Lu-PSMA-I&T [97], while the response rate was 40% in a larger cohort [166]. Median progression-free survival was 4 months, and median overall survival was 13 months [166], and these correlated with > 30% PSA decline at week 6 [167]. In comparison to ^{177}Lu-PSMA-617, the whole-body and tumor half-lives of ^{177}Lu-PSMA-I&T were lower [168]. Notwithstanding these pharmacokinetic differences, mean absorbed tumor doses were comparable for the two radioligands [168]. Absorbed dose in parotid, submandibular, and lacrimal glands is comparable or slightly lower for ^{177}Lu-PSMA-I&T [168], but dose to kidneys is elevated [168,169]. Both radiopharmaceuticals are well-tolerated, with grade 1/2 xerostomia and small, but statistically significant, reductions in hemoglobin, platelet counts, and leukocyte counts the primary toxicities [166,168]. On the basis of these favorable characteristics, ^{225}Ac-PSMA-I&T has undergone preliminary evaluation in a small cohort of patients with mCRPC [170]. Initial findings confirmed efficacy even in patients refractory to β-particle therapy [170,171] with grade 1 or 2 xerostomia the most commonly reported side effect. The characteristics of these compounds, as well as other leading ligands to advance to clinical evaluation, are summarized in Table 1.

Radiohalogenated PSMA inhibitors for theranostics

The identification of a number of potent small molecule inhibitors of PSMA containing iodophenyl [172], iodobenzyl [173] or iodobenzamide groups [85,174] has stimulated the development of alternatives to MIP-1095 for PSMA-targeted theranostics. Although comparisons between molecules evaluated in different xenograft models should be performed with caution, it appears that the tumor-to-kidney ratio of these radiohalogenated ligands is generally lower than that of MIP-1095 [172–174]. Consequently, although Auger electron-emitting ^{125}I-DCIBzL and α-particle-emitting ^{211}At-DCAtBzL are efficacious in micrometastatic prostate cancer animal models, the therapeutic effect was observed only at doses associated with delayed renal toxicity [175,176]. Attempts to improve the pharmacokinetics of ^{211}At-labeled compounds for targeted alpha particle therapy identified one compound, [^{211}At]HS-549, with superior tumor-to-kidney ratios in mice, but this is

Table 1
Comparison of the most clinically advanced theranostic PSMA ligands on the basis of clinical status, most significant attributes and most significant detriments. Representative clinical trial identifiers are reported where applicable.

Compound	Clinical Status	Significant Attributes	Significant Detriments	Refs.
J591	^{89}Zr: Phase I/II ^{177}Lu: Phase II (NCT00195039)	• 95% accuracy for bone lesions • Non-immunogenic • Response is proportional to PSMA expression	• 60% accuracy for soft tissue lesions • Dose-limiting, but reversible, hematological toxicity due to prolonged circulation • Modest therapeutic (any PSA decline) response compared to small molecule ligands	145 147
	^{225}Ac: Phase I/II (NCT04506567)	• Effective in patients that received ^{177}Lu-J591 as prior therapy • No grade 3/4 hematological toxicity	• Lower tumor penetration	148, 149
PSMA-617	^{68}Ga: Phase I	• High sensitivity and specificity (> 87%)	• Slower renal clearance than ^{68}Ga-PSMA-11 • Intense salivary gland uptake	152,153
	^{44}Sc: First-in-Human	• Tumor SUV is similar to ^{68}Ga-PSMA-11 • Tumor imaging possible up to 18 h, providing better match for ^{177}Lu dosimetry calculations	• Dose to kidneys is 2x higher than ^{68}Ga-PSMA-617	212
	^{64}Cu: First-in-Human	• Late stage PET imaging (2 $h < t <$ 22 h) is possible	• No additional lesions are evident at later imaging time points • Radiation dose is higher than ^{68}Ga ligands • Limited *in vivo* stability	203
	^{177}Lu: FDA Approved (2022)	• Response rate is 45–55% with no grade 3/4 toxicities	• Relapse is frequent • Dose-dependent xerostomia	154–162
	^{225}Ac: Phase I (NCT04597411)	• Response rate >60% even in patients refractory to ^{177}Lu-PSMA-617 • No hematological toxicity	• Dose-limiting xerostomia • Delayed nephrotoxicity possible	94,95,163,164
PSMA-I&T	^{177}Lu: Phase III (NCT05204927)	• Lower whole body $t_{1/2}$ than ^{177}Lu-PSMA-617 • Lower dose to parotid, submandibular, and lacrimal glands than ^{177}Lu-PSMA-617	• Shorter tumor $t_{1/2}$ than ^{177}Lu-PSMA-617 • Higher kidney dose than ^{177}Lu-PSMA-617	97,166–169
	^{225}Ac: First-in-Human	• Tumor response achieved in patients refractory to ^{177}Lu-PSMA-I&T	• Grade 1/2 xerostomia	170,171
^{131}I-MIP-1095	Phase II (NCT03939689)	• >65% response to a single dose	• Dose-limiting xerostomia • Relapse is frequent • No improvement in tumor response upon subsequent doses	82, 93
^{177}Lu-PSMA-ALB-56	First-in-Human	• Higher dose in tumor lesions than ^{177}Lu-PSMA-617 and ^{177}Lu-PSMA-i&T • Lower kidney dose than other albumin-binding ligands	• Kidney and red marrow doses are higher than ^{177}Lu-PSMA-617 • Dose to salivary glands is comparable to ^{177}Lu-PSMA-617	192
^{177}Lu-EB-PSMA-617	Phase I (NCT03403595)	• Comparable response to ^{177}Lu-PSMA-617 at lower administered dose	• Substantially higher salivary gland dose than ^{177}Lu-PSMA-617 • Dose-dependent hematological toxicity	190, 191

likely due to extensive dehalogenation of this compound which renders it unattractive for clinical translation [177]. Even where the kidney absorbed dose is lower than that observed with MIP-1095, as is the case for MIP-1072, accumulation of the ligand in tumors is also significantly decreased [151], and further clinical evaluation is not warranted.

One exception to this trend is the iodophenyl ligand, RPS-027 [85]. This small molecule dually targets both PSMA and serum albumin to increase tumor accumulation as a function of increased plasma residence time. As a result, the tumor-to-kidney ratio in preclinical models is superior to that of other radiohalogenated PSMA ligands. RPS-027 validated the strategy of incorporating albumin-binding moieties into PSMA-binding structures to increase the therapeutic index. Despite a promising pharmacokinetic profile, the major limitation of RPS-027 and its structural analogues is the inability to independently modify PSMA affinity and albumin affinity. Further optimization of this class of molecules was not possible.

Albumin-binding PSMA ligands for theranostics

Next generation PSMA theranostic ligands have separated the albumin-binding moiety and the PSMA-binding moiety in chemical space, often using a linker group to which a macrocyclic chelator is conjugated. This modular approach has allowed the relative affinities for PSMA and serum albumin to be fine-tuned. The advantages to such an approach are evident in ^{177}Lu-RPS-063, which delivers 5 times greater dose to tumors than ^{177}Lu-PSMA-617 in an LNCaP xenograft tumor model [178]. Notwithstanding the high PSMA affinity and the affinity for serum albumin, clearance from blood is faster than expected, and clearance of activity from tumors is evident after 4 h post injection. Extended tumor loading and retention is achieved by using ^{177}Lu-RPS-072, in which the high affinity 4-(4-iodophenyl)butanoic acid (IPBA) albumin binding group [179] increases affinity for serum albumin, with a corresponding delay in the clearance from blood [180]. In concert with an increasing dose to LNCaP tumors, 1.5 times greater than ^{177}Lu-RPS-063 over 96 h, is a significant reduction in kidney retention. The resulting tumor-to-kidney ratio compares favorably to other ligands evaluated in an LNCaP xenograft model. Clearance from blood fits an exponential decay function with a half-life of 14.6 h [180]. By comparison, pharmacokinetic modeling in human patients has shown the plasma clearance of ^{177}Lu-J591 to be an exponential decay function with a half-life of 39.1 ± 13.3 h [181]. These data suggest that enhanced albumin binding is unlikely to lead to dose-limiting hematologic toxicity and support the application of this platform to TAT. RPS-074 [182] is a structural analogue of RPS-072 that employs the macropa [183] macrocyclic chelator for ^{225}Ac chelation. A complete tumor response with no overt toxicity was observed in an LNCaP xenograft model following a single dose of 148 kBq ^{225}Ac-RPS-074, with a single dose of 74 kBq allowing tumor control over 6 weeks [182].

As an alternative to the modular trifunctional constructs, many groups have explored albumin-binding derivatives of PSMA-617. These compounds incorporate a range of albumin binding moieties, including the higher affinity IPBA [184,185], 4-(4-chlorophenyl)butyric acid [186], ibuprofen [187,188], and Evans blue (EB) [189] groups, and the moderate affinity *p*-(tolyl)butanoic acid [87] moiety. Activity in PC3-PIP xenograft tumors is high and sustained following injection of these ligands, leading to an area under the curve (AUC) that is 2–5 times greater than for ^{177}Lu-PSMA-617 in the same model [87,184,[186,189]]. This trend is also observed in an LNCaP xenograft model [185,186]. This is significant because the expression level of PSMA in PC3-PIP cells is 10-fold higher than in LNCaP cells [175] and likely is substantially higher than expression in clinical samples. Activity in the kidney is also substantially higher and persists up to 192 h post injection. One exception is ^{177}Lu-PSMA-ALB-56, which exhibits a steeper clearance curve [87]. PSMA-ALB-56 incorporates a lower affinity albumin binding group, although the relationship between serum albumin binding and kidney clearance requires further study. Tumor control is accomplished for 5–9 weeks following a single dose of the ^{177}Lu-labeled ligand with no apparent toxicity [189]. This translates to survival benefits in xenograft mouse models. Encouragingly, preliminary clinical head-to-head evaluation of these ^{177}Lu-labeled albumin-binding PSMA ligands against ^{177}Lu-PSMA-617 indicates 2–3 times greater absorbed dose in tumors [190] and translates to adequate tumor control without grade 3 or 4 toxicities [191]. Kidney [190,192] and red marrow [191,192] doses are also increased, however. The longer-term implications of these off-target doses are under investigation.

The EB group has also been used to increase the circulation time of a small molecule incorporating a glutamate-urea-cysteine moiety for PSMA binding rather than a glutamate-urea-lysine moiety [193]. Despite comparable affinity for PSMA, uptake of ^{90}Y-DOTA-EB-MCG in PC3-PIP xenograft tumors is reduced relative to that observed with ^{86}Y-EB-PSMA-617 [193]. A construct conjugating a phosphoramidate-based PSMA binding group and IPBA to the DOTA macrocycle obtained by click chemistry slowly clears from the blood, leading to progressive tumor loading [194]. Although accumulation of this molecule, ^{177}Lu-CTT1403, in PC3-PIP tumors is sustained beyond 120-h post injection, activity in the kidney is high at all time-points. As a result, the tumor-to-kidney ratio does not exceed 1 [195], and renal toxicity will likely limit the dose that can be safely administered.

It is argued that conjugation of an albumin binding group to a PSMA targeting ligand decreases the rate of renal excretion due to a reduction in receptor-mediated kidney uptake [194], perhaps as a consequence of masking the highly anionic charge of the molecule. Early preclinical experience with albumin-binding PSMA ligands is inconclusive in this regard: some compounds with high albumin binding exhibit relatively low kidney doses (e.g., ^{177}Lu-RPS-072, ^{177}Lu-PSMA-ALB-56, ^{177}Lu-I-bu-DAB-PSMA), while others demonstrate prolonged kidney retention. The consequences of renal retention on nephrotoxicity arising from targeted radioligand therapy have yet to be determined, but this activity can be displaced by administration of 2-(phosphonomethyl)pentanedioic acid (2-PMPA) [84], a potent PSMA inhibitor [196], or non-radiolabeled PSMA-11 [197], a small molecule PSMA inhibitor [198,199] that is FDA-approved for prostate cancer imaging when labeled with ^{68}Ga. Nor is it established whether enhanced albumin binding will restrict physiological uptake of radiolabeled PSMA ligands in submandibular, parotid, and lacrimal glands. Assessment of ligand uptake in these tissues in preclinical murine models is challenging, in part because the rodent glands are substantially different from those of humans. Clinical data are scarce but conflicting; increased circulation time of [^{18}F]DCFBC [200] relative to [^{18}F]DCFPyL [130] corresponds with decreased gland uptake, but accumulation of ^{177}Lu-EB-PSMA-617 in these glands is more pronounced than that obtained with ^{177}Lu-PSMA-617 [190], and the albumin-binding compound ^{177}Lu-L14 accumulates in salivary glands to a greater extent than analogous PSMA ligands with faster blood clearance in a preclinical model [201]. Further evaluation of albumin-binding PSMA ligands in prostate cancer patients may resolve this outstanding question.

Application of novel radionuclides, radioisotopes, and chelators to PSMA theranostics

In tandem with the development of new PSMA targeting ligands is the use of emerging radionuclides for imaging and therapy and the development of novel chelators to complex these metals. Radioisotopes of copper are re-emerging for theranostic application in prostate cancer. Copper-64 ($t_{1/2}$ = 12.7 h, β^+ = 18%, β^- = 39%) is itself a theranostic ligand, and also forms a unique theranostic pair with ^{67}Cu ($t_{1/2}$ = 2.58 d, β^- = 100%). Preliminary evaluation of ^{64}Cu-PSMA-617 in prostate cancer patients revealed accumulation of activity in the liver, indicating insufficient complex stability [202,203]. Consequently, PSMA targeting molecules bearing chelators that complex copper with greater stability are in preclinical development. Early examples of these chelators cleared rapidly from circulation, leading to low uptake in xenograft tumors

[204,205]. Subsequently, constructs incorporating albumin binding groups have been described. ^{64}Cu-PSMA-ALB-89, a NODAGA-containing analogue of PSMA-ALB-56, accumulates in both PC3-PIP xenografts and kidneys [206], while ^{64}Cu-RPS-085, a derivative of RPS-063 bearing a sarcophagine chelator, clears more rapidly from kidneys [207]. In comparison to other copper-labeled radioligands, in particular PSMA-617, activity in the liver following administration of ^{64}Cu-RPS-085 [207] or the bivalent sarcophagine inhibitor ^{64}Cu-SarbisPSMA [208] is very low. This is evidence of the high stability of copper chelation by the sarcophagine moiety. With a sarcophagine-conjugated octreotate molecule currently undergoing clinical trial for imaging and targeted radioligand therapy in neuroendocrine cancer [209] and a single 30 MBq dose of ^{67}Cu-SarbisPSMA achieving tumor control for 6 weeks [210], there is great potential for the application of sarcophagine chelators to PSMA-based theranostics.

The $^{43/44/47}$Sc theranostic triad also holds promise in clinical management of prostate cancer. The physical properties of ^{43}Sc ($t_{1/2}$ = 3.89 h, β^+ = 88%), ^{44}Sc ($t_{1/2}$ = 4.04 h, β^+ = 95%) and ^{47}Sc ($t_{1/2}$ = 3.35 d, β^- = 100%) are better suited for radioligands with longer circulation times, such as albumin-binding PSMA ligands, than ^{68}Ga [211]. Of the two positron-emitting isotopes of scandium, ^{43}Sc is preferred for clinical application because ^{44}Sc has a high energy gamma emission that increases radiation dose [212]. Initial studies of ^{44}Sc-PSMA-617 confirm PSMA-specific uptake and high complex stability with distribution kinetics similar to ^{177}Lu-PSMA-617 [213,214]. First-in-human evaluations suggest that dosimetry is favorable to ^{177}Lu-PSMA-617 in the context of pre-therapy planning [213]. However, chelation of Sc^{3+} by DOTA requires prolonged heating at 95 °C. Consequently, new chelators have been introduced that complex Sc^{3+} rapidly and under mild conditions. One such example is picaga, a small bifunctional heterocyclic chelator with a picolinate arm that forms highly stable complexes with Sc^{3+} and Lu^{3+} [215]. A single dose of ^{177}Lu-picaga-Alb53-PSMA inhibited tumor growth for more than 3 weeks in a preclinical prostate cancer model [216]. Greater efficacy may be possible with a multiple dose regimen, although the effect of dose fractionation on off-target toxicity is yet to be established.

As new radiometal β-emitters for PSMA-targeted radioligand therapy, such as ^{47}Sc [216,217], ^{67}Cu 207,208,210], and ^{161}Tb [218], and α-emitters, such as ^{149}Tb [219], ^{212}Pb [220,221], ^{227}Th [222], and ^{225}Ac become more widely available, the value of bifunctional chelators capable of rapidly complexing metal ions with high *in vivo* stability will continue to grow. This is particularly true for TAT, in which release of the radiometal from the chelator can lead to dose-limiting toxicity as a result of undesirable accumulation of the free metal in off-target tissue. Despite its widespread use, the DOTA macrocycle is not optimal for larger α-emitters such as actinium-225. This is evidenced by the decrease in lanthanide-DOTA complex stability constant with increasing lanthanide ion diameter [223]. The lack of stability is likely a product of both small ring size and the distance between the metal ion and the oxygen donor atoms of the acetic acid pendant arms [224]. To address these limitations, larger 18-membered macrocycles such as macropa [183], crown [225], py-macrodipa [226], and mcp-D-click [227] have recently been introduced to chelate $^{225}Ac^{3+}$ or $^{213}Bi^{3+}$ with exceptionally high stability. An alternative approach has been to explore acyclic hydroxypyridinonate (HOPO) or picolinic acid chelators. To date, these chelators have been used to complex Th^{4+} with reasonable stability [228,229]. The development of these novel chelators, along with those reported for Sc^{3+} [215,217], Cu^{2+} [208], Lu^{3+} [215], and Pb^{2+} [230], represents an exciting development in PSMA theranostics. Nevertheless, many of these chelators have yet to be prepared and tested as bifunctional conjugates, and their incorporation into high affinity PSMA targeting ligands remains to be demonstrated.

Salivary gland PSMA as a barrier to the development of PSMA-based theranostics: strategies and hypotheses for future treatment

Accumulation of PSMA ligands in the major salivary glands represent a major barrier for targeted radiotherapy of prostate cancer. This accumulation is comparable to the sequestration of PSMA ligands within the diseased prostate and results in irreversible damage to the glands [94,95]. These glands produce saliva and loss of this production significantly impacts the quality-of-life of patients receiving targeted radiotherapy with certain PSMA ligands [231,232]. Early, unsuccessful, strategies for reducing sialotoxicity targeted inflammation and included approaches such as external cooling of the glands with ice packs [233, 234], and sialendoscopy with steroid injection [235]. These experiences confirmed that xerostomia was not caused by inflammation alone. More promising results were obtained with the intraparenchymal injection of botulinum toxin, which significantly reduced PSMA ligand uptake in the treated parotid gland [236]. More recent studies have shown that higher doses of this toxin are tolerated [237]. However, this approach is based on disruption of the neural control of the treated gland and so is limited to the injected glands only and may cause extended dysfunction of gland activity.

The mixed results of these initial experiences have stimulated interest in understanding and perturbing the mechanism of uptake and sequestration of PSMA ligands by salivary glands. Aside from the PSMA specific antibodies, J591 and 7E11-C5.3, most PSMA ligands are small molecule anions due in part for the requirement of a glutamyl residue for binding the PSMA active site. Many of these ligands therefore include a glutamate moiety and numerous groups have sought to displace these ligands using glutamate [238–240]. Intraperitoneal injection of monosodium glutamate (MSG) reduced salivary gland and kidney uptake of ^{68}Ga-PSMA-11 in mice without significantly altering tumor uptake [238]. Although the rationale for the approach is the displacement of ^{68}Ga-PSMA-11 by glutamate, this mechanism is not the most likely explanation for the observed reductions in salivary gland and kidney retention. Glutamate is rapidly metabolized in the gut upon first pass [241], meaning that the mass available for ^{68}Ga-PSMA-11 antagonism in kidneys and salivary glands is substantially reduced. By contrast, the mass of sodium administered, $>$ 45 mg/kg at the effective dose of MSG, translates to an increase in blood sodium concentration of $>$ 25 mM. Physiological sodium concentration is highly regulated, and hypernatremia on this scale is likely to induce thirst, changes in sympathetic nerve activity, release of antidiuretic hormones [242], and reduced salivary gland flow rates [243] to restore sodium concentration. Notwithstanding these observations, co-administration of MSG is being investigated in two clinical trials designed to reduce uptake of ^{68}Ga-PSMA-11 (NCT04282824) or ^{18}F-DCFPyL (NCT03693742) uptake for imaging.

We wish to propose the process by which organic anions are transported from blood and concentrated in saliva as an alternative target for intervention. Daily saliva production varies between 0.5 and 1.5 liters in humans and is facilitated by the transepithelial transport of ions [244]. A comprehensive account of saliva and its constituents is beyond the scope of this review (instead see [244,245]), instead we will discuss two anions: thiocyanate, $[SCN]^-$ and nitrate, NO_3^-, concentrated in saliva—and by extension within the salivary glands—to both indicate the unique actions of these glands and a possible means by which they sequester PSMA ligands.

$[SCN]^-$ arises from the actions of rhodanese (EC 2.8.1.1) on cyanide (CN^-), which is released during the catabolism of many foods or inhaled as a component of combusted tobacco and marijuana [246,247]. In addition to being significantly less toxic than CN^-, $[SCN]^-$ is the preferred substrate for myeloperoxidase (EC 1.11.2.2) and salivary peroxidase (EC 1.11.1.7), both of which exist in saliva [248]. These enzymes catalyze the oxidation of halides and $[SCN]^-$ to their respective hypohalous acids (e.g., hypochlorous acid and hypothiocyanous acid) as a part of the oral antimicrobial defense [249–251]. $[SCN]^-$ is

remarkably concentrated in saliva relative to serum (1 mM vs. 34 μM [252,253], and reaching 2.6 mM in smokers [253]). NO_3^- is similarly concentrated by the salivary glands from serum for secretion as a salivary anion. The concentrations of NO_3^- in blood and saliva are 38 μM and 435 μM, respectively [254,255]. Salivary glands act to recover 25% of the NO_3^- in blood and return it to the cardiovascular system to support the production of nitric oxide, is a critical modulator of vascular relaxation [256]. Salivary NO_3^- concentrations vary as a function of age and diet and can be increased as much as 100-fold relative to blood NO_3^- levels by dietary supplementation [256,257]. Thus, salivary glands act to sequester anions from the blood and in some cases, such as $[SCN]^-$ and NO_3^-, concentrate these for secretion into saliva to support oral and general health.

Sialin is a versatile anion transporter expressed in salivary glands [258] that transports glutamate, NO_3^-, and other anions from blood to saliva. We hypothesize that salivary epithelium sequesters the PSMA ligands by uptake through the sialin anion/H^+ symporter on the basolateral side of these cells but is not able to secrete the ligands into the saliva at the apical side. This imbalance between the ingress and egress of PSMA ligands results in their accumulation. In support of this hypothesis, sialin transports NAAG and a variety of glutamate containing xenobiotics, as well as NO_3^- and glutamate, into epithelial cells [259–261]. Salivary glands also express the most sialin in mammals [258,261] whereas the other conduit for PSMA ligand uptake, PSMA, is expressed at very low levels in these glands [10,36,89]. Moreover, PSMA expression is restricted to intercalated epithelium of these glands [36]. Intercalated epithelial cells constitute a relatively minor portion of salivary gland and explains the apparent absence of PSMA in some studies [19,91,262]. The role of PSMA in the intercalated epithelia cells is not known, but interestingly these cells give rise to neoplasias just as the PSMA expressing cells in the prostate do [263,264].

Uptake of small molecule PSMA ligands by salivary sialin/H^+ symporters suggest the possibility of antagonizing this uptake and sparing the salivary glands during targeted radiotherapy. Possible antagonists include sialin transport inhibitors developed by Gasnier and colleagues [259,265], oral poly-glutamate tablets [239,240], and anions concentrated by the salivary glands like NO_3^- and $[SCN]^-$. The advantages of the NO_3^- as salivary PSMA ligand antagonists include the availability of numerous medically approved formulations this anion, and the fact that NO_3^- is radioprotective [257]. Humans also tolerate $[SCN]^-$ well (as indicated by smokers) and this compound can act as an antioxidant [266–268]. Intriguingly, a recent study in patients receiving radiotherapy for oropharyngeal cancer identified an inverse correlation between smoking and the grade of xerostomia [269], and these patients are likely to have had nM concentrations of $[SCN]^-$ in their blood. We are not aware of meta-analyses of prostate cancer patients receiving PSMA radioligand therapy that investigate this relationship. Additionally, radiotherapy for nasopharyngeal carcinoma results in long term and significant decrements in salivary NO_3^- and $[SCN]^-$ levels [270]. Thus, augmenting the salivary concentrations of these anions, prior to targeted radiotherapy, may produce salutary effects in addition to mitigating salivary PSMA ligand uptake [257]. Testing these possibilities would be best done using miniature pigs, which unlike rodents, have parotid glands that resemble those of humans [271,272].

Conclusions and future directions

Over the past decade, the theranostic paradigm has driven ligand development for PSMA-targeted imaging and therapy. This effort has seen the translation of multiple PSMA-targeting ligands for imaging and radioligand therapy of mCRPC. Given the expression of PSMA is non-prostatic neoplasms, there may also be an opportunity for PSMA-targeted imaging and therapy in non-prostatic disease [273]. If this proves to be the case, the clinical experience with PSMA theranostics in mCRPC patients will be invaluable. The impact of ligands such as J591, PSMA-617, and PSMA-I&T to extending life with quality is already considerable, and these ligands have also provided crucial information about tissue distribution and off-target toxicity. Consequently, emerging ligands complexing new radionuclides are poised to address the limitations of the first generation theranostic compounds. One of the major limitations is salivary gland toxicity, which is prevalent and may even be irreversible in TAT. The mechanism of uptake of small molecule PSMA ligands in the salivary glands is not yet known, but strategies for their displacement are emerging. It remains to be seen if these strategies are effective in reducing long-term salivary gland toxicity.

As clinical experience with TAT continues to grow, it will be necessary to address the challenges of performing dosimetry for new PSMA ligands. The versatility of DOTA enables dosimetry for ^{225}Ac-labeled constructs to be estimated on the basis of the tissue distribution of the ^{177}Lu-labeled ligand. However, in the absence of stable isotopes of actinium, it is often difficult to determine whether the PSMA affinity of the ^{225}Ac-labeled and ^{177}Lu-labeled analogues are identical. As a result, there is inherent uncertainty in these estimates of dosimetry. New chelating moieties that chelate Ac^{3+} with greater stability may transform TAT and increase the therapeutic index of the ligands to which they are conjugated. However, these chelating moieties may be highly selective for Ac^{3+}, thereby preventing the use of chemically identical ligands labeled with radiometals such as $^{111}In^{3+}$ and $^{177}Lu^{3+}$ for estimating dosimetry. Substitution of another chelating moiety for the purposes of binding smaller radiometals might influence the tissue distribution of the ligand, adding further uncertainty to the dosimetry calculations. New strategies will need to be developed in order to fully capitalize on the potential of PSMA TAT.

In addition to highlighting the challenges of producing and assessing the PSMA ligands as theranostic agents, we have sought to note areas where biology might aid in these efforts. Most, if not all, ligands are based on compounds that block the catalytic activity of PSMA – and more to the point – the hydrolysis of *N*-acetyl aspartylglutamate. This strategy favors the regulation of *N*-acetyl-a-linked dipeptidase. The actions of PSMA in prostate cancer may be to endocytose folates and therefore rely on different molecular interactions than those required to hydrolyze peptide linkages. Given that the efficacy of PSMA ligands as prostate cancer theranostics relies on the endocytosis of these compounds, a better understanding of this process is likely to lead to better therapeutics. This effort will also be aided by identifying the ligands for PSMA in prostate cancer, as these compounds will serve as parent compounds of future ligands. Identifying these ligands also has the potential of identifying potential risk factors for this disease. Since one of the candidates for the endogenous prostatic PSMA ligand is folic acid, these studies are of interest not only to those of us wishing to eliminate prostate cancer, but a broader community whose purvey includes public health and policy.

CRediT authorship contribution statement

Thomas M. Jeitner: Conceptualization, Writing – original draft, Writing – review & editing. **John W. Babich:** Conceptualization, Writing – original draft, Writing – review & editing. **James M. Kelly:** Conceptualization, Writing – original draft, Writing – review & editing, Resources.

Declaration of Competing Interest

J.W. Babich and J.M. Kelly hold intellectual property rights to compounds described in this manuscript. J.W. Babich and J.M. Kelly also hold equity in Ratio Therapeutics, a licensor of intellectual property related to compounds described in this manuscript. T.M. Jeitner has no declarations of interest to disclose.

Acknowledgments

Mr. Brendan Murphy and Prof. John T. Pinto and Arthur J.L. Cooper

are thanked for their careful editing of the manuscript, as well as their insightful suggestions.

References

[1] C.H. Halsted, E.H. Ling, R. Luthi-Carter, J.A. Villanueva, J.M. Gardner, J.T. Coyle, Folylpoly-gamma-glutamate carboxypeptidase from pig jejunum. Molecular characterization and relation to glutamate carboxypeptidase II, J. Biol. Chem. 273 (32) (1998) 20417–20424. Aug 7.

[2] R. Luthi-Carter, A.K. Barczak, H. Speno, J.T. Coyle, Molecular characterization of human brain N-acetylated alpha-linked acidic dipeptidase (NAALADase), J. Pharmacol. Exp. Ther. 286 (2) (1998) 1020–1025. Aug.

[3] G.L. Wright, C. Haley, M.L. Beckett, P.F. Schellhammer, Expression of prostate-specific membrane antigen in normal, benign, and malignant prostate tissues, Urol. Oncol. 1 (1) (1995) 18–28. Feb.

[4] A.M. Reisenauer, C.H. Halsted, Human jejunal brush border folate conjugase. Characteristics and inhibition by salicylazosulfapyridine, Biochim. Biophys. Acta (BBA) Enzymol. 659 (1) (1981) 62–69. May.

[5] B.H. Maraj, J.P. Leek, M. Karayi, M. Ali, N.J. Lench, A.F. Markham, Detailed genetic mapping around a putative prostate-specific membrane antigen locus on human chromosome 11p11.2, Cytogenet. Cell Genet. 81 (1) (1998) 3–9.

[6] D.S. O'Keefe, S.L. Su, D.J. Bacich, Y. Horiguchi, Y. Luo, C.T. Powell, et al., Mapping, genomic organization and promoter analysis of the human prostate-specific membrane antigen gene, Biochim. Biophys. Acta (BBA) Gene Struct. Expr. 1443 (1–2) (1998) 113–127. Nov.

[7] J. Leek, N. Lench, B. Maraj, A. Bailey, I.M. Carr, S. Andersen, et al., Prostate-specific membrane antigen: evidence for the existence of a second related human gene, Br. J. Cancer 72 (3) (1995) 583–588. Sep.

[8] C. Barinka, P. Sácha, J. Sklenár, P. Man, K. Bezouska, B.S. Slusher, et al., Identification of the N-glycosylation sites on glutamate carboxypeptidase II necessary for proteolytic activity, Protein Sci. 13 (6) (2004) 1627–1635. Jun.

[9] T. Williams, R. Kole, Analysis of prostate-specific membrane antigen splice variants in LNCap cells, Oligonucleotides 16 (2) (2006) 186–195.

[10] R.S. Israeli, C.T. Powell, W.R. Fair, W.D. Heston, Molecular cloning of a complementary DNA encoding a prostate-specific membrane antigen, Cancer Res. 53 (2) (1993) 227–230. Jan 15.

[11] P. Mlcochová, C. Barinka, J. Tykvart, P. Sácha, J. Konvalinka, Prostate-specific membrane antigen and its truncated form PSM, Prostate 69 (5) (2009) 471–479. Apr 1.

[12] X. Zhang, C. Morrissey, S. Sun, M. Ketchandji, P.S. Nelson, L.D. True, et al., Androgen receptor variants occur frequently in castration resistant prostate cancer metastases, PLoS One 6 (11) (2011) e27970. Nov 17.

[13] S. Divyya, S.M. Naushad, A. Addlagatta, P.V.L.N. Murthy, C.R. Reddy, R. R. Digumarti, et al., Paradoxical role of C1561T glutamate carboxypeptidase II (GCPII) genetic polymorphism in altering disease susceptibility, Gene 497 (2) (2012) 273–279. Apr 15.

[14] S.F. Altschul, T.L. Madden, A.A. Schäffer, J. Zhang, Z. Zhang, W. Miller, et al., Gapped BLAST and PSI-BLAST: a new generation of protein database search programs, Nucleic Acids Res. 25 (17) (1997) 3389–3402. Sep 1.

[15] R. Luthi-Carter, U.V. Berger, A.K. Barczak, M. Enna, J.T. Coyle, Isolation and expression of a rat brain cDNA encoding glutamate carboxypeptidase II, Proc. Natl. Acad. Sci. USA 95 (6) (1998) 3215–3220. Mar 17.

[16] M.B. Robinson, R.D. Blakely, R. Couto, J.T. Coyle, Hydrolysis of the brain dipeptide N-acetyl-L-aspartyl-L-glutamate. Identification and characterization of a novel N-acetylated alpha-linked acidic dipeptidase activity from rat brain, J. Biol. Chem. 262 (30) (1987) 14498–14506. Oct 25.

[17] T.D. Schmittgen, S. Teske, R.L. Vessella, L.D. True, B.A. Zakrajsek, Expression of prostate specific membrane antigen and three alternatively spliced variants of PSMA in prostate cancer patients, Int. J. Cancer 107 (2) (2003) 323–329. Nov 1.

[18] L.S. Grauer, K.D. Lawler, J.L. Marignac, A. Kumar, A.S. Goel, R.L. Wolfert, Identification, purification, and subcellular localization of prostate-specific membrane antigen PSM' protein in the LNCaP prostatic carcinoma cell line, Cancer Res. 58 (21) (1998) 4787–4789. Nov 1.

[19] D.A. Silver, I. Pellicer, W.R. Fair, W.D. Heston, Cordon-Cardo C. Prostate-specific membrane antigen expression in normal and malignant human tissues, Clin. Cancer Res. 3 (1) (1997) 81–85. Jan.

[20] A. Ghosh, W.D.W. Heston, Tumor target prostate specific membrane antigen (PSMA) and its regulation in prostate cancer, J. Cell. Biochem. 91 (3) (2004) 528–539. Feb 15.

[21] J.L. Kasperzyk, S.P. Finn, R. Flavin, M. Fiorentino, R. Lis, W.K. Hendrickson, et al., Prostate-specific membrane antigen protein expression in tumor tissue and risk of lethal prostate cancer, Cancer Epidemiol. Biomark. Prev. 22 (12) (2013) 2354–2363. Dec.

[22] A. Bychkov, U. Vutrapongwatana, S. Tepmongkol, S. Keelawat, PSMA expression by microvasculature of thyroid tumors - potential implications for PSMA theranostics, Sci. Rep. 7 (1) (2017) 5202. Jul 12.

[23] P. Mahzouni, M. Shavakhi, Prostate-specific membrane antigen expression in neovasculature of glioblastoma multiforme, Adv. Biomed. Res. 8 (2019) 18. Feb 27.

[24] Y. Tolkach, H. Gevensleben, R. Bundschuh, A. Koyun, D. Huber, C. Kehrer, et al., Prostate-specific membrane antigen in breast cancer: a comprehensive evaluation of expression and a case report of radionuclide therapy, Breast Cancer Res. Treat. 169 (3) (2018) 447–455. Jun.

[25] A.G. Wernicke, S. Kim, H. Liu, N.H. Bander, E.C. Pirog, Prostate-specific membrane antigen (PSMA) expression in the neovasculature of gynecologic malignancies: implications for PSMA-targeted therapy, Appl. Immunohistochem. Mol. Morphol. 25 (4) (2017) 271–276. Apr.

[26] H. Wang, S. Wang, W. Song, Y. Pan, H. Yu, T. Si, et al., Expression of prostate-specific membrane antigen in lung cancer cells and tumor neovasculature endothelial cells and its clinical significance, PLoS One 10 (5) (2015), e0125924. May 15.

[27] M. Abdel-Hadi, Y. Ismail, L Younis, Prostate-specific membrane antigen (PSMA) immunoexpression in the neovasculature of colorectal carcinoma in Egyptian patients, Pathol. Res. Pract. 210 (11) (2014) 759–763. Nov.

[28] M.C. Haffner, I.E. Kronberger, J.S. Ross, C.E. Sheehan, M. Zitt, G. Mühlmann, et al., Prostate-specific membrane antigen expression in the neovasculature of gastric and colorectal cancers, Hum. Pathol. 40 (12) (2009) 1754–1761. Dec.

[29] M.C. Haffner, J. Laimer, A. Chaux, G. Schäfer, P. Obrist, A. Brunner, et al., High expression of prostate-specific membrane antigen in the tumor-associated neovasculature is associated with worse prognosis in squamous cell carcinoma of the oral cavity, Mod. Pathol. 25 (8) (2012) 1079–1085. Aug.

[30] A. Gatto, L. Falvo, S. Sebastiani, G. Roncolini, G. Pinna, Triple synchronous tumours of the urinary system with different histologies: a case report, Chir. Ital. 61 (3) (2009) 381–385. Jun.

[31] A. Baccala, L. Sercia, J. Li, W. Heston, M. Zhou, Expression of prostate-specific membrane antigen in tumor-associated neovasculature of renal neoplasms, Urology 70 (2) (2007) 385–390. Aug.

[32] B.S. Slusher, M.B. Robinson, G. Tsai, M.L. Simmons, S.S. Richards, J.T. Coyle, Rat brain N-acetylated alpha-linked acidic dipeptidase activity. Purification and immunologic characterization, J. Biol. Chem. 265 (34) (1990) 21297–21301. Dec 5.

[33] B.S. Slusher, G. Tsai, G. Yoo, J.T. Coyle, Immunocytochemical localization of the N-acetyl-aspartyl-glutamate (NAAG) hydrolyzing enzyme N-acetylated alpha-linked acidic dipeptidase (NAALADase), J. Comp. Neurol. 315 (2) (1992) 217–229. Jan 8.

[34] U.V. Berger, R.E. Carter, M. McKee, J.T. Coyle, N-acetylated alpha-linked acidic dipeptidase is expressed by non-myelinating Schwann cells in the peripheral nervous system, J. Neurocytol. 24 (2) (1995) 99–109. Feb.

[35] M. Rovenská, K. Hlouchová, P. Sácha, P. Mlcochová, V. Horák, J. Zámecník, et al., Tissue expression and enzymologic characterization of human prostate specific membrane antigen and its rat and pig orthologs, Prostate 68 (2) (2008) 171–182. Feb 1.

[36] N.J. Rupp, C.A. Umbricht, D.A. Pizzuto, D. Lenggenhager, A. Töpfer, J. Müller, et al., First clinicopathologic evidence of a Non-PSMA-related uptake mechanism for 68Ga-PSMA-11 in salivary glands, J. Nucl. Med. 60 (9) (2019) 1270–1276. Sep.

[37] F. Watt, A. Martorana, D.E. Brookes, T. Ho, E. Kingsley, D.S. O'Keefe, et al., A tissue-specific enhancer of the prostate-specific membrane antigen gene, FOLH1, Genomics 73 (3) (2001) 243–254. May 1.

[38] S.J. Lee, K. Lee, X. Yang, C. Jung, T. Gardner, H.S. Kim, et al., NFATc1 with AP-3 site binding specificity mediates gene expression of prostate-specific-membrane-antigen, J. Mol. Biol. 330 (4) (2003) 749–760. Jul 18.

[39] W. Peng, L. Guo, R. Tang, X. Liu, R. Jin, J..T. Dong, et al., Sox7 negatively regulates prostate-specific membrane antigen (PSMA) expression through PSMA-enhancer, Prostate 79 (4) (2019) 370–378. Mar.

[40] C. Sulidankazha, W. Han, T. He, H. Lin, K. Cheng, X. Nie, et al., miR-146a inhibited pancreatic cancer cell proliferation by targeting SOX7, J. Healthc. Eng. (2022), 2240605, 2022 Feb 16.

[41] L. Guo, D. Zhong, S. Lau, X. Liu, X.Y. Dong, X. Sun, et al., Sox7 Is an independent checkpoint for beta-catenin function in prostate and colon epithelial cells, Mol. Cancer Res. 6 (9) (2008) 1421–1430. Sep.

[42] N.D. Rawlings, A.J. Barrett, Structure of membrane glutamate carboxypeptidase, Biochim. Biophys. Acta (BBA)Protein Struct. Mol. Enzymol. 1339 (2) (1997) 247–252. May.

[43] J.R. Mesters, C. Barinka, W. Li, T. Tsukamoto, P. Majer, B.S. Slusher, et al., Structure of glutamate carboxypeptidase II, a drug target in neuronal damage and prostate cancer, EMBO J. 25 (6) (2006) 1375–1384. Mar 22.

[44] R.D. Blakely, M.B. Robinson, R.C. Thompson, J.T. Coyle, Hydrolysis of the brain dipeptide N-acetyl-L-aspartyl-L-glutamate: subcellular and regional distribution, ontogeny, and the effect of lesions on N-acetylated-alpha-linked acidic dipeptidase activity, J. Neurochem. 50 (4) (1988) 1200–1209. Apr.

[45] J.H. Neale, R. Olszewski, A role for N-acetylaspartylglutamate (NAAG) and mGluR3 in cognition, Neurobiol. Learn. Mem. 158 (2019) 9–13. Feb.

[46] J.J. Vornov, K.R. Hollinger, P.F. Jackson, K.M. Wozniak, M.H. Farah, P. Majer, et al., Still naag'ing after all these years: the continuing pursuit of GCPII inhibitors, Adv. Pharmacol. 76 (2016) 215–255. Mar 18.

[47] T. Bzdega, S.L. Crowe, E.R. Ramadan, K.H. Sciarretta, R.T. Olszewski, O.A. Ojeifo, et al., The cloning and characterization of a second brain enzyme with NAAG peptidase activity, J. Neurochem. 89 (3) (2004) 627–635. May.

[48] K. Hlouchová, C. Barinka, V. Klusák, P. Sácha, P. Mlcochová, P. Majer, et al., Biochemical characterization of human glutamate carboxypeptidase III, J. Neurochem. 101 (3) (2007) 682–696. May.

[49] R. Wang, P.H. Reddy, Role of glutamate and NMDA receptors in alzheimer's disease, J. Alzheimers Dis. 57 (4) (2017) 1041–1048.

[50] P. Khacho, B. Wang, N. Ahlskog, E. Hristova, R. Bergeron, Differential effects of N-acetyl-aspartyl-glutamate on synaptic and extrasynaptic NMDA receptors are subunit- and pH-dependent in the CA1 region of the mouse hippocampus, Neurobiol. Dis. 82 (2015) 580–592. Oct.

[51] A.J.L. Cooper, T.M. Jeitner, Central role of glutamate metabolism in the maintenance of nitrogen homeostasis in normal and hyperammonemic brain, Biomolecules 6 (2) (2016) 16. Mar 26.

[52] K.A. Rahn, B.S. Slusher, A.I. Kaplin, Glutamate in CNS neurodegeneration and cognition and its regulation by GCPII inhibition, Curr. Med. Chem. 19 (9) (2012) 1335–1345.

[53] J.J. Vornov, D. Peters, M. Nedelcovych, K. Hollinger, R. Rais, B.S. Slusher, Looking for drugs in all the wrong places: use of GCPII inhibitors outside the brain, Neurochem. Res. 45 (6) (2020) 1256–1267. Jun.

[54] L.E. Jin, M. Wang, V.C. Galvin, T.C. Lightbourne, P.J. Conn, A.F.T. Arnsten, et al., mGluR2 versus mGluR3 metabotropic glutamate receptors in primate dorsolateral prefrontal cortex: postsynaptic mglur3 strengthen working memory networks, Cereb. Cortex 28 (3) (2018) 974–987. Mar 1.

[55] K.R. Hollinger, A. Sharma, C. Tallon, L. Lovell, A.G. Thomas, X. Zhu, et al., Dendrimer-2PMPA selectively blocks upregulated microglial GCPII activity and improves cognition in a mouse model of multiple sclerosis, Nanotheranostics 6 (2) (2022) 126–142. Jan 1.

[56] C.F. Zink, P.B. Barker, A. Sawa, D.R. Weinberger, M. Wang, H. Quillian, et al., Association of missense mutation in FOLH1 with decreased NAAG levels and impaired working memory circuitry and cognition, Am. J. Psychiatry 177 (12) (2020) 1129–1139. Dec 1.

[57] D. Datta, S.N. Leslie, E. Woo, N. Amancharla, A. Elmansy, M. Lepe, et al., Glutamate carboxypeptidase II in aging rat prefrontal cortex impairs working memory performance, Front. Aging Neurosci. 13 (2021), 760270. Nov 15.

[58] U.V. Berger, R.E. Carter, J.T. Coyle, The immunocytochemical localization of N-acetylaspartyl glutamate, its hydrolysing enzyme NAALADase, and the NMDAR-1 receptor at a vertebrate neuromuscular junction, Neuroscience 64 (4) (1995) 847–850. Feb.

[59] P. Marmiroli, B. Slusher, G. Cavaletti, Tissue distribution of glutamate carboxypeptidase II (GCPII) with a focus on the central and peripheral nervous system, Curr. Med. Chem. 19 (9) (2012) 1277–1281.

[60] Z. Zhang, B. Bassam, A.G. Thomas, M. Williams, J. Liu, E. Nance, et al., Maternal inflammation leads to impaired glutamate homeostasis and up-regulation of glutamate carboxypeptidase II in activated microglia in the fetal/newborn rabbit brain, Neurobiol. Dis. 94 (2016) 116–128. Oct.

[61] O. Arteaga Cabeza, Z. Zhang, E. Smith Khoury, R.A. Sheldon, A. Sharma, F. Zhang, et al., Neuroprotective effects of a dendrimer-based glutamate carboxypeptidase inhibitor on superoxide dismutase transgenic mice after neonatal hypoxic-ischemic brain injury, Neurobiol. Dis. 148 (2021), 105201. Jan.

[62] D. Ha, S.J. Bing, G. Ahn, J. Kim, J. Cho, A. Kim, et al., Blocking glutamate carboxypeptidase II inhibits glutamate excitotoxicity and regulates immune responses in experimental autoimmune encephalomyelitis, FEBS J. 283 (18) (2016) 3438–3456. Sep.

[63] A.A. Simen, K.A. Bordner, M.P. Martin, L.A. Moy, L.C. Barry, Cognitive dysfunction with aging and the role of inflammation, in: Ther Adv Chronic Dis, 2, 2011, pp. 175–195. May.

[64] B.P. Ramos, S.G. Birnbaum, I. Lindenmayer, S.S. Newton, R.S. Duman, A.F. T. Arnsten, Dysregulation of protein kinase a signaling in the aged prefrontal cortex: new strategy for treating age-related cognitive decline, Neuron 40 (4) (2003) 835–845. Nov 13.

[65] K.J. Carpenter, S. Sen, E.A. Matthews, S.L. Flatters, K.M. Wozniak, B.S. Slusher, et al., Effects of GCP-II inhibition on responses of dorsal horn neurones after inflammation and neuropathy: an electrophysiological study in the rat, Neuropeptides 37 (5) (2003) 298–306. Oc.

[66] F. Scaglione, G. Panzavolta, Folate, folic acid and 5-methyltetrahydrofolate are not the same thing, Xenobiotica 44 (5) (2014) 480–488. May.

[67] C.M. Pfeiffer, J.P. Hughes, D.A. Lacher, R.L. Bailey, R.J. Berry, M. Zhang, et al., Estimation of trends in serum and RBC folate in the U.S. population from pre- to postfortification using assay-adjusted data from the NHANES 1988-2010, J. Nutr. 142 (5) (2012) 886–893. May.

[68] C.M. Pfeiffer, M.R. Sternberg, Z. Fazili, D.A. Lacher, M. Zhang, C.L. Johnson, et al., Folate status and concentrations of serum folate forms in the US population: national Health and Nutrition Examination Survey 2011-2, Br. J. Nutr. 113 (12) (2015) 1965–1977. Jun 28.

[69] D.P. Nguyen, P.L. Xiong, H. Liu, S. Pan, W. Leconet, V. Navarro, et al., Induction of PSMA and Internalization of an Anti-PSMA mAb in the vascular compartment, Mol. Cancer Res. 14 (11) (2016) 1045–1053. Nov.

[70] J. Cardinale, M. Schäfer, M. Benešová, U. Bauder-Wüst, K. Leotta, M. Eder, et al., Preclinical evaluation of 18F-PSMA-1007, a new prostate-specific membrane antigen ligand for prostate cancer imaging, J. Nucl. Med. 58 (3) (2017) 425–431. Mar.

[71] G. Anilkumar, S.A. Rajasekaran, S. Wang, O. Hankinson, N.H. Bander, A. K. Rajasekaran, Prostate-specific membrane antigen association with filamin a modulates its internalization and NAALADase activity, Cancer Res. 63 (10) (2003) 2645–2648. May 15.

[72] S. Schmidt, B. Gericke, G. Fracasso, D. Ramarli, M. Colombatti, H.Y. Naim, Discriminatory role of detergent-resistant membranes in the dimerization and endocytosis of prostate-specific membrane antigen, PLoS One 8 (6) (2013) e66193. Jun 19.

[73] M.I. Davis, M.J. Bennett, L.M. Thomas, P.J. Bjorkman, Crystal structure of prostate-specific membrane antigen, a tumor marker and peptidase, Proc. Natl. Acad. Sci. USA 102 (17) (2005) 5981–5986. Apr 26.

[74] S. Barua, K. Rege, Cancer-cell-phenotype-dependent differential intracellular trafficking of unconjugated quantum dots, Small 5 (3) (2009) 370–376. Mar.

[75] J.F. Presley, S. Mayor, T.E. McGraw, K.W. Dunn, F.R. Maxfield, Bafilomycin A1 treatment retards transferrin receptor recycling more than bulk membrane recycling, J. Biol. Chem. 272 (21) (1997) 13929–13936. May 23.

[76] A.C.M. DeGroot, D.J. Busch, C.C. Hayden, S.A. Mihelic, A.T. Alpar, M. Behar, et al., Entropic control of receptor recycling using engineered ligands, Biophys. J. 114 (6) (2018) 1377–1388. Mar 27.

[77] V. Yao, C.E. Berkman, J.K. Choi, D.S. O'Keefe, D.J Bacich, Expression of prostate-specific membrane antigen (PSMA), increases cell folate uptake and proliferation and suggests a novel role for PSMA in the uptake of the non-polyglutamated folate, folic acid, Prostate 70 (3) (2010) 305–316. Feb 15.

[78] H. Birn, O. Spiegelstein, E.I. Christensen, R.H. Finnell, Renal tubular reabsorption of folate mediated by folate binding protein 1, J. Am. Soc. Nephrol. 16 (3) (2005) 608–615. Mar.

[79] H.A. Al-Ahmadie, S. Olgac, P.D. Gregor, S.K. Tickoo, S.W. Fine, G.V. Kondagunta, et al., Expression of prostate-specific membrane antigen in renal cortical tumors, Mod. Pathol. 21 (6) (2008) 727–732. Jun.

[80] J.T. Pinto, B.P. Suffoletto, T.M. Berzin, C.H. Qiao, S. Lin, W.P. Tong, et al., Prostate-specific membrane antigen: a novel folate hydrolase in human prostatic carcinoma cells, Clin. Cancer Res. 2 (9) (1996) 1445–1451. Sep.

[81] W.C. Winkelmayer, C. Eberle, G. Sunder-Plassmann, M. Födinger, Effects of the glutamate carboxypeptidase II (GCP2 1561C>T) and reduced folate carrier (RFC1 80G>A) allelic variants on folate and total homocysteine levels in kidney transplant patients, Kidney Int. 63 (6) (2003) 2280–2285. Jun.

[82] C.M. Zechmann, A. Afshar-Oromieh, T. Armor, J.B. Stubbs, W. Mier, B. Hadaschik, et al., Radiation dosimetry and first therapy results with a (124)I/(131)I-labeled small molecule (MIP-1095) targeting PSMA for prostate cancer therapy, Eur. J. Nucl. Med. Mol. Imaging 41 (7) (2014) 1280–1292. Jul.

[83] S. Vallabhajosula, A. Nikolopoulou, J.W. Babich, J.R. Osborne, S.T. Tagawa, I. Lipai, et al., ^{99m}Tc-labeled small-molecule inhibitors of prostate-specific membrane antigen: pharmacokinetics and biodistribution studies in healthy subjects and patients with metastatic prostate cancer, J. Nucl. Med. 55 (11) (2014) 1791–1798. Nov.

[84] C. Kratochwil, F.L. Giesel, K. Leotta, M. Eder, T. Hoppe-Tich, H. Youssoufian, et al., PMPA for nephroprotection in PSMA-targeted radionuclide therapy of prostate cancer, J. Nucl. Med. 56 (2) (2015) 293–298. Feb.

[85] J.M. Kelly, A. Amor-Coarasa, A. Nikolopoulou, T. Wüstemann, P. Barelli, D. Kim, et al., Dual-target binding ligands with modulated pharmacokinetics for endoradiotherapy of prostate cancer, J. Nucl. Med. 58 (9) (2017) 1442–1449. Sep.

[86] M. Benešová, M. Schäfer, U. Bauder-Wüst, A. Afshar-Oromieh, C. Kratochwil, W. Mier, et al., Preclinical evaluation of a tailor-made DOTA-conjugated PSMA inhibitor with optimized linker moiety for imaging and endoradiotherapy of prostate cancer, J. Nucl. Med. 56 (6) (2015) 914–920. Jun.

[87] C.A. Umbricht, M. Benešová, R. Schibli, C. Müller, Preclinical development of novel PSMA-targeting radioligands: modulation of albumin-binding properties to improve prostate cancer therapy, Mol. Pharm. 15 (6) (2018) 2297–2306. Jun 4.

[88] S. Ray Banerjee, M. Pullambhatla, C.A. Foss, A. Falk, Y. Byun, S. Nimmagadda, et al., Effect of chelators on the pharmacokinetics of (99 m)Tc-labeled imaging agents for the prostate-specific membrane antigen (PSMA), J. Med. Chem. 56 (15) (2013) 6108–6121. Aug 8.

[89] J.K. Troyer, M.L. Beckett, G.L. Wright, Detection and characterization of the prostate-specific membrane antigen (PSMA) in tissue extracts and body fluids, Int. J. Cancer 62 (5) (1995) 552–558. Sep 4.

[90] P. Wolf, N. Freudenberg, P. Bühler, K. Alt, W. Schultze-Seemann, U. Wetterauer, et al., Three conformational antibodies specific for different PSMA epitopes are promising diagnostic and therapeutic tools for prostate cancer, Prostate 70 (5) (2010) 562–569. Apr 1.

[91] P. Mhawech-Fauceglia, S. Zhang, L. Terracciano, G. Sauter, A. Chadhuri, F. R. Herrmann, et al., Prostate-specific membrane antigen (PSMA) protein expression in normal and neoplastic tissues and its sensitivity and specificity in prostate adenocarcinoma: an immunohistochemical study using mutiple tumour tissue microarray technique, Histopathology 50 (4) (2007) 472–483. Mar.

[92] W.P. Fendler, S. Reinhardt, H. Ilhan, A. Delker, G. Böning, F.J. Gildehaus, et al., Preliminary experience with dosimetry, response and patient reported outcome after 177Lu-PSMA-617 therapy for metastatic castration-resistant prostate cancer, Oncotarget 8 (2) (2017) 3581–3590. Jan 10.

[93] A. Afshar-Oromieh, U. Haberkorn, C. Zechmann, T. Armor, W. Mier, F. Spohn, et al., Repeated PSMA-targeting radioligand therapy of metastatic prostate cancer with 131I-MIP-1095, Eur. J. Nucl. Med. Mol. Imaging 44 (6) (2017) 950–959. Jun.

[94] C. Kratochwil, F. Bruchertseifer, F.L. Giesel, M. Weis, F.A. Verburg, F. Mottaghy, et al., ^{225}Ac-PSMA-617 for PSMA-targeted α-radiation therapy of metastatic castration-resistant prostate cancer, J. Nucl. Med. 57 (12) (2016) 1941–1944. Dec.

[95] C. Kratochwil, F. Bruchertseifer, H. Rathke, M. Bronzel, C. Apostolidis, W. Weichert, et al., Targeted α-therapy of metastatic castration-resistant prostate cancer with ^{225}Ac-PSMA-617: dosimetry estimate and empiric dose finding, J. Nucl. Med. 58 (10) (2017) 1624–1631. Oct.

[96] R. Tönnesmann, P.T. Meyer, M. Eder, A.C. Baranski, [^{177}Lu]Lu-PSMA-617 salivary gland uptake characterized by quantitative *in vitro* autoradiography, Pharm. (Basel) 12 (1) (2019) 18. Jan 24.

[97] R.P. Baum, H.R. Kulkarni, C. Schuchardt, A. Singh, M. Wirtz, S. Wiessalla, et al., ^{177}Lu-labeled prostate-specific membrane antigen radioligand therapy of metastatic castration-resistant prostate cancer: safety and efficacy, J. Nucl. Med. 57 (7) (2016) 1006–1013. Jul.

[98] H. Ahmadzadehfar, E. Eppard, S. Kürpig, R. Fimmers, A. Yordanova, C. D. Schlenkhoff, et al., Therapeutic response and side effects of repeated radioligand therapy with ^{177}Lu-PSMA-DKFZ-617 of castrate-resistant metastatic prostate cancer, Oncotarget 7 (11) (2016) 12477–12488. Mar 15.

[99] K. Rahbar, M. Boegemann, A. Yordanova, M. Eveslage, M. Schäfers, M. Essler, et al., PSMA targeted radioligandtherapy in metastatic castration resistant prostate cancer after chemotherapy, abiraterone and/or enzalutamide. A retrospective analysis of overall survival, Eur. J. Nucl. Med. Mol. Imaging 45 (1) (2018) 12–19. Jan.
[100] D.S. O'Keefe, D.J. Bacich, S.S. Huang, W.D.W. Heston, A perspective on the evolving story of PSMA biology, PSMA-based imaging, and endoradiotherapeutic strategies, J. Nucl. Med. 59 (7) (2018) 1007–1013. Jul.
[101] S. Raz, M. Stark, Y.G. Assaraf, Folylpoly-γ-glutamate synthetase: a key determinant of folate homeostasis and antifolate resistance in cancer, Drug Resist. Updat. 28 (2016) 43–64. Sep.
[102] B. Shane, High performance liquid chromatography of folates: identification of poly-gamma-glutamate chain lengths of labeled and unlabeled folates, Am. J. Clin. Nutr. 35 (3) (1982) 599–608. Mar.
[103] I. Eto, C.L. Krumdieck, Determination of three different pools of reduced one-carbon-substituted folates. III. Reversed-phase high-performance liquid chromatography of the azo dye derivatives of p-aminobenzoylpoly-γ-glutamates and its application to the study of unlabeled endogenous pteroylpolyglutamates of rat liver, Anal. Biochem. 120 (2) (1982) 323–329. Mar.
[104] C. Kaittanis, C. Andreou, H. Hieronymus, N. Mao, C.A. Foss, M. Eiber, et al., Prostate-specific membrane antigen cleavage of vitamin B9 stimulates oncogenic signaling through metabotropic glutamate receptors, J. Exp. Med. 215 (1) (2018) 159–175. Jan 2.
[105] K. He, R. Marsland, S. Upadhyayula, E. Song, S. Dang, B.R. Capraro, et al., Dynamics of phosphoinositide conversion in clathrin-mediated endocytic traffic, Nature 552 (7685) (2017) 410–414. Dec 21.
[106] K.T. Aung, K. Yoshioka, S. Aki, K. Ishimaru, N. Takuwa, Y. Takuwa, The class II phosphoinositide 3-kinases PI3K-C2α and PI3K-C2β differentially regulate clathrin-dependent pinocytosis in human vascular endothelial cells, J. Physiol. Sci. 69 (2) (2019) 263–280. Mar.
[107] C.R. Reis, P.H. Chen, S. Srinivasan, F. Aguet, M. Mettlen, S.L. Schmid, Crosstalk between Akt/GSK3β signaling and dynamin-1 regulates clathrin-mediated endocytosis, EMBO J. 34 (16) (2015) 2132–2146. Aug 13.
[108] D. Leyton-Puig, T. Isogai, E. Argenzio, B. van den Broek, J. Klarenbeek, H. Janssen, et al., Flat clathrin lattices are dynamic actin-controlled hubs for clathrin-mediated endocytosis and signalling of specific receptors, Nat. Commun. 8 (2017) 16068. Jul 13.
[109] E. Schneider, T.J. Ryan, Gamma-glutamyl hydrolase and drug resistance, Clin. Chim. Acta 374 (1–2) (2006) 25–32. Dec.
[110] M. Tio, J. Andrici, M.R. Cox, G.D. Eslick, Folate intake and the risk of prostate cancer: a systematic review and meta-analysis, Prostate Cancer Prostatic Dis. 17 (3) (2014) 213–219. Sep.
[111] K.J. Rycyna, D.J. Bacich, D.S. O'Keefe, Divergence between dietary folate intake and concentrations in the serum and red blood cells of aging males in the United States, Clin. Nutr. 35 (4) (2016) 928–934. Aug.
[112] S.C. Tinker, H.C. Hamner, Y.P. Qi, K.S. Crider, U.S. women of childbearing age who are at possible increased risk of a neural tube defect-affected pregnancy due to suboptimal red blood cell folate concentrations, National Health and Nutrition Examination Survey 2007 to 2012, Birth Defects Res. Part A Clin. Mol. Teratol. 103 (6) (2015) 517–526. Jun.
[113] S.L. Boulet, Q. Yang, C. Mai, R.S. Kirby, J.S. Collins, J.M. Robbins, et al., Trends in the postfortification prevalence of spina bifida and anencephaly in the United States, Birth Defects Res. Part A Clin. Mol. Teratol. 82 (7) (2008) 527–532. Jul.
[114] C.A.M. Atta, K.M. Fiest, A.D. Frolkis, N. Jette, T. Pringsheim, C. St Germaine-Smith, et al., Global birth prevalence of spina bifida by folic acid fortification status: a systematic review and meta-analysis, Am. J. Public Health 106 (1) (2016) e24–e34. Jan.
[115] M.R. Sweeney, J. McPartlin, J. Scott, Folic acid fortification and public health: report on threshold doses above which unmetabolised folic acid appear in serum, BMC Public Health 7 (2007) 41. Mar 22.
[116] P. Kelly, J. McPartlin, M. Goggins, D.G. Weir, J.M. Scott, Unmetabolized folic acid in serum: acute studies in subjects consuming fortified food and supplements, Am. J. Clin. Nutr. 65 (6) (1997) 1790–1795. Jun.
[117] S.W. Bailey, J.E. Ayling, The extremely slow and variable activity of dihydrofolate reductase in human liver and its implications for high folic acid intake, Proc. Natl. Acad. Sci. USA 106 (36) (2009) 15424–15429. Sep 8.
[118] C.Z. Palchetti, C. Paniz, E. de Carli, D.M. Marchioni, C. Colli, J. Steluti, et al., Association between serum unmetabolized folic acid concentrations and folic acid from fortified foods, J. Am. Coll. Nutr. 36 (7) (2017) 572–578. Oct.
[119] L. Plumptre, S.P. Masih, A. Ly, S. Aufreiter, K.J. Sohn, R. Croxford, et al., High concentrations of folate and unmetabolized folic acid in a cohort of pregnant Canadian women and umbilical cord blood, Am. J. Clin. Nutr. 102 (4) (2015) 848–857. Oct.
[120] R. Obeid, S.H. Kirsch, M. Kasoha, R. Eckert, W. Herrmann, Concentrations of unmetabolized folic acid and primary folate forms in plasma after folic acid treatment in older adults, Metab. Clin. Exp. 60 (5) (2011) 673–680. May.
[121] N. Wang, J.A. McCammon, Substrate channeling between the human dihydrofolate reductase and thymidylate synthase, Protein Sci. 25 (1) (2016) 79–86. Jan.
[122] R. Nilsson, M. Jain, N. Madhusudhan, N.G. Sheppard, L. Strittmatter, C. Kampf, et al., Metabolic enzyme expression highlights a key role for MTHFD2 and the mitochondrial folate pathway in cancer, Nat. Commun. 5 (2014) 3128.
[123] D. Smith, J. Hornstra, M. Rocha, G. Jansen, Y. Assaraf, I. Lasry, et al., Folic acid impairs the uptake of 5-methyltetrahydrofolate in human umbilical vascular endothelial cells, J. Cardiovasc. Pharmacol. 70 (4) (2017) 271–275. Oct.
[124] A. Cimadamore, M. Cheng, M. Santoni, A. Lopez-Beltran, N. Battelli, F. Massari, et al., New prostate cancer targets for diagnosis, imaging, and therapy: focus on prostate-specific membrane antigen, Front. Oncol. 8 (2018) 653. Dec 21.
[125] E. Gourni, G. Henriksen, Metal-based PSMA radioligands, Molecules 22 (4) (2017). Mar 24.
[126] C. Kesch, C. Kratochwil, W. Mier, K. Kopka, Giesel FL. 68 ga or 18F for prostate cancer imaging? J. Nucl. Med. 58 (5) (2017) 687–688. May.
[127] S. Piron, J. Verhoeven, C. Vanhove, F. De Vos, Recent advancements in 18F-labeled PSMA targeting PET radiopharmaceuticals, Nucl. Med. Biol. 106–107 (2022) 29–51. Apr.
[128] H.J. Wester, M. Schottelius, PSMA-targeted radiopharmaceuticals for imaging and therapy, Semin. Nucl. Med. 49 (4) (2019) 302–312. Jul.
[129] A. Afshar-Oromieh, A. Malcher, M. Eder, M. Eisenhut, H.G. Linhart, B. A. Hadaschik, et al., PET imaging with a [68Ga]gallium-labelled PSMA ligand for the diagnosis of prostate cancer: biodistribution in humans and first evaluation of tumour lesions, Eur. J. Nucl. Med. Mol. Imaging 40 (4) (2013) 486–495. Apr.
[130] Z. Szabo, E. Mena, S.P. Rowe, D. Plyku, R. Nidal, M.A. Eisenberger, et al., Initial evaluation of [(18)F]DCFPyL for prostate-specific membrane antigen (PSMA)-targeted PET imaging of prostate cancer, Mol. Imaging Biol. 17 (4) (2015) 565–574. Aug.
[131] S.C. Behr, R. Aggarwal, H.F. VanBrocklin, R.R. Flavell, K. Gao, E.J. Small, et al., Phase I study of CTT1057, an 18F-labeled imaging agent with phosphoramidate core targeting prostate-specific membrane antigen in prostate cancer, J. Nucl. Med. 60 (7) (2019) 910–916. Jul.
[132] F.L. Giesel, B. Hadaschik, J. Cardinale, J. Radtke, M. Vinsensia, W. Lehnert, et al., F-18 labelled PSMA-1007: biodistribution, radiation dosimetry and histopathological validation of tumor lesions in prostate cancer patients, Eur. J. Nucl. Med. Mol. Imaging 44 (4) (2017) 678–688. Apr.
[133] F.L. Giesel, K. Knorr, F. Spohn, L. Will, T. Maurer, P. Flechsig, et al., Detection efficacy of 18F-PSMA-1007 PET/CT in 251 patients with biochemical recurrence of prostate cancer after radical prostatectomy, J. Nucl. Med. 60 (3) (2019) 362–368. Mar.
[134] F. Dietlein, M. Hohberg, C. Kobe, B.D. Zlatopolskiy, P. Krapf, H. Endepols, et al., An 18F-labeled PSMA ligand for PET/CT of prostate cancer: first-in-humans observational study and clinical experience with 18F-JK-PSMA-7 during the first year of application, J. Nucl. Med. 61 (2) (2020) 202–209. Feb.
[135] M. Hohberg, C. Kobe, P. Krapf, P. Täger, J. Hammes, F. Dietlein, et al., Biodistribution and radiation dosimetry of [18F]-JK-PSMA-7 as a novel prostate-specific membrane antigen-specific ligand for PET/CT imaging of prostate cancer, EJNMMI Res. 9 (1) (2019) 66. Jul 25.
[136] H. Rathke, A. Afshar-Oromieh, F.L. Giesel, C. Kremer, P. Flechsig, S. Haufe, et al., Intraindividual comparison of 99mTc-methylene diphosphonate and prostate-specific membrane antigen ligand 99mTc-MIP-1427 in patients with osseous metastasized prostate cancer, J. Nucl. Med. 59 (9) (2018) 1373–1379. Sep.
[137] J.B. Ćwikła, M. Roslan, I. Skoneczna, M. Kempińska-Wróbel, M. Maurin, W. Rogowski, et al., Initial experience of clinical use of [99mTc]Tc-PSMA-T4 in patients with prostate cancer. A pilot study, Pharmaceuticals 14 (11) (2021). BaselOct 29.
[138] P. Werner, C. Neumann, M. Eiber, H.J. Wester, M. Schottelius, [99cmTc]Tc-PSMA-I&S-SPECT/CT: experience in prostate cancer imaging in an outpatient center, EJNMMI Res. 10 (1) (2020) 45. May 7.
[139] F. García-Pérez, J. Davanzo, S. López-Buenrostro, C. Santos-Cuevas, G. Ferro-Flores, M. Jímenez-Ríos, et al., Original article head to head comparison performance of 99mTc-EDDA/HYNIC-iPSMA SPECT/CT and, Am. J. Nucl. Med. Mol. Imaging 8 (5) (2018) 332–340.
[140] A. Wurzer, D. Di Carlo, A. Schmidt, R. Beck, M. Eiber, M. Schwaiger, et al., Radiohybrid Ligands: a novel tracer concept exemplified by 18F- or 68Ga-labeled rhPSMA inhibitors, J. Nucl. Med. 61 (5) (2020) 735–742. May.
[141] S. Malaspina, P. Taimen, M. Kallajoki, V. Oikonen, A. Kuisma, O. Ettala, et al., Uptake of 18F-rhPSMA-7.3 in positron emission tomography imaging of prostate cancer: a phase 1 proof-of-concept study, Cancer Biother. Radiopharm. 37 (3) (2022) 205–213. Apr.
[142] D. Kahn, R.D. Williams, M.J. Manyak, M.K. Haseman, D.W. Seldin, J.A. Libertino, et al., 111Indium-capromab pendetide in the evaluation of patients with residual or recurrent prostate cancer after radical prostatectomy. The ProstaScint study group, J. Urol. 159 (6) (1998) 2041–2046. Jundiscussion 2046.
[143] D.M. Nanus, M.I. Milowsky, L. Kostakoglu, P.M. Smith-Jones, S. Vallabahajosula, S.J. Goldsmith, et al., Clinical use of monoclonal antibody HuJ591 therapy: targeting prostate specific membrane antigen, J. Urol. 170 (2003) S84–S88. Dec6 Pt 2)discussion S88.
[144] M.J. Morris, N. Pandit-Taskar, C.R. Divgi, S. Bender, J.A. O'Donoghue, A. Nacca, et al., Phase I evaluation of J591 as a vascular targeting agent in progressive solid tumors, Clin. Cancer Res. 13 (9) (2007) 2707–2713. May 1.
[145] N. Pandit-Taskar, J.A. O'Donoghue, J.C. Durack, S.K. Lyashchenko, S.M. Cheal, V. Beylergil, et al., A phase I/II study for analytic validation of 89Zr-J591 immunoPET as a molecular imaging agent for metastatic prostate cancer, Clin. Cancer Res. 21 (23) (2015) 5277–5285. Dec 1.
[146] M.I. Milowsky, D.M. Nanus, L. Kostakoglu, S. Vallabhajosula, S.J. Goldsmith, N. H. Bander, Phase I trial of yttrium-90-labeled anti-prostate-specific membrane antigen monoclonal antibody J591 for androgen-independent prostate cancer, J. Clin. Oncol. 22 (13) (2004) 2522–2531. Jul 1.
[147] S.T. Tagawa, M.I. Milowsky, M. Morris, S. Vallabhajosula, P. Christos, N. H. Akhtar, et al., Phase II study of lutetium-177-labeled anti-prostate-specific membrane antigen monoclonal antibody J591 for metastatic castration-resistant prostate cancer, Clin. Cancer Res. 19 (18) (2013) 5182–5191. Sep 15.

[148] S.T. Tagawa, S. Vallabhajosula, Y. Jhanwar, K.V. Ballman, A. Hackett, L. Emmerich, et al., Phase I dose-escalation study of^{225} Ac-J591 for progressive metastatic castration resistant prostate cancer (mCRPC), J. Clin. Oncol. 36 (2018). TPS399–TPS399, Feb 20(6_suppl).

[149] S.T. Tagawa, M. Sun, A.O. Sartor, C. Thomas, S. Singh, M. Bissassar, et al., Phase I study of^{225} Ac-J591 for men with metastatic castration-resistant prostate cancer (mCRPC), JCO 39 (2021) 5015. May 20(15_suppl)–5015.

[150] A.P. Kozikowski, F. Nan, P. Conti, J. Zhang, E. Ramadan, T. Bzdega, et al., Design of remarkably simple, yet potent urea-based inhibitors of glutamate carboxypeptidase II (NAALADase), J. Med. Chem. 44 (3) (2001) 298–301. Feb 1.

[151] J.A. Barrett, R.E. Coleman, S.J. Goldsmith, S. Vallabhajosula, N.A. Petry, S. Cho, et al., First-in-man evaluation of 2 high-affinity PSMA-avid small molecules for imaging prostate cancer, J. Nucl. Med. 54 (3) (2013) 380–387. Mar.

[152] A. Afshar-Oromieh, H. Hetzheim, C. Kratochwil, M. Benesova, M. Eder, O. C. Neels, et al., The theranostic PSMA Ligand PSMA-617 in the diagnosis of prostate cancer by PET/CT: biodistribution in humans, radiation dosimetry, and first evaluation of tumor lesions, J. Nucl. Med. 56 (11) (2015) 1697–1705. Nov 1.

[153] Y. Li, D. Han, P. Wu, J. Ren, S. Ma, J. Zhang, et al., Comparison of 68Ga-PSMA-617 PET/CT with mpMRI for the detection of PCa in patients with a PSA level of 4-20ng/ml before the initial biopsy, Sci. Rep. 10 (1) (2020) 10963. Jul 3.

[154] J. Violet, P. Jackson, J. Ferdinandus, S. Sandhu, T. Akhurst, A. Iravani, et al., Dosimetry of 177Lu-PSMA-617 in metastatic castration-resistant prostate cancer: correlations between pretherapeutic imaging and whole-body tumor dosimetry with treatment outcomes, J. Nucl. Med. 60 (4) (2019) 517–523. Apr.

[155] L. Emmett, M. Crumbaker, B. Ho, K. Willowson, P. Eu, L. Ratnayake, et al., Results of a prospective phase 2 pilot trial of 177Lu-PSMA-617 therapy for metastatic castration-resistant prostate cancer including imaging predictors of treatment response and patterns of progression, Clin. Genitourin. Cancer 17 (1) (2019) 15–22. Feb.

[156] Y.J. Kim, Y.I. Kim, Therapeutic responses and survival effects of 177Lu-PSMA-617 radioligand therapy in metastatic castrate-resistant prostate cancer: a meta-analysis, Clin. Nucl. Med. 43 (10) (2018) 728–734. Oct.

[157] M.P. Yadav, S. Ballal, R.K. Sahoo, M. Tripathi, N.A. Damle, S.A. Shamim, et al., Long-term outcome of 177Lu-PSMA-617 radioligand therapy in heavily pre-treated metastatic castration-resistant prostate cancer patients, PLoS One 16 (5) (2021), e0251375. May 10.

[158] K. Rahbar, A. Afshar-Oromieh, H. Jadvar, H. Ahmadzadehfar, PSMA theranostics: current status and future directions, Mol. Imaging 17 (2018). Dec, doi: 1536012118776068.

[159] J. Calais, A. Gafita, M. Eiber, W.R. Armstrong, J. Gartmann, P. Thin, et al., Prospective phase 2 trial of PSMA-targeted molecular RadiothErapy with 177Lu-PSMA-617 for metastatic castration-reSISTant prostate cancer (RESIST-PC): efficacy results of the UCLA cohort, J. Nucl. Med. 62 (10) (2021) 1440–1446. Oct.

[160] O. Sartor, J. de Bono, K.N. Chi, K. Fizazi, K. Herrmann, K. Rahbar, et al., Lutetium-177-PSMA-617 for metastatic castration-resistant prostate cancer, N. Engl. J. Med. 385 (12) (2021) 1091–1103. Sep 16.

[161] K. Rahbar, A. Bode, M. Weckesser, N. Avramovic, M. Claesener, L. Stegger, et al., Radioligand therapy with 177Lu-PSMA-617 as a novel therapeutic option in patients with metastatic castration resistant prostate cancer, Clin. Nucl. Med. 41 (7) (2016) 522–528. Jul.

[162] M.S. Hofman, J. Violet, R.J. Hicks, J. Ferdinandus, S.P. Thang, T. Akhurst, et al., [177Lu]-PSMA-617 radionuclide treatment in patients with metastatic castration-resistant prostate cancer (LuPSMA trial): a single-centre, single-arm, phase 2 study, Lancet Oncol. 19 (6) (2018) 825–833. Jun.

[163] C. Kratochwil, F. Bruchertseifer, H. Rathke, M. Hohenfellner, F.L. Giesel, U. Haberkorn, et al., Targeted α-therapy of metastatic castration-resistant prostate cancer with 225Ac-PSMA-617: swimmer-plot analysis suggests efficacy regarding duration of tumor control, J. Nucl. Med. 59 (5) (2018) 795–802. May.

[164] M. Sathekge, F. Bruchertseifer, O. Knoesen, F. Reyneke, I. Lawal, T. Lengana, et al., 225Ac-PSMA-617 in chemotherapy-naive patients with advanced prostate cancer: a pilot study, Eur. J. Nucl. Med. Mol. Imaging 46 (1) (2019) 129–138. Jan.

[165] M.M. Sathekge, F. Bruchertseifer, I.O. Lawal, M. Vorster, O. Knoesen, T. Lengana, et al., Treatment of brain metastases of castration-resistant prostate cancer with 225Ac-PSMA-617, Eur. J. Nucl. Med. Mol. Imaging 46 (8) (2019) 1756–1757. Jul.

[166] M.M. Heck, R. Tauber, S. Schwaiger, M. Retz, C. D'Alessandria, T. Maurer, et al., Treatment outcome, toxicity, and predictive factors for radioligand therapy with 177Lu-PSMA-I&T in metastatic castration-resistant prostate cancer, Eur. Urol. 75 (6) (2019) 920–926. Jun.

[167] A. Gafita, M.M. Heck, I. Rauscher, R. Tauber, L. Cala, C. Franz, et al., Early prostate-specific antigen changes and clinical outcome after 177Lu-PSMA radionuclide treatment in patients with metastatic castration-resistant prostate cancer, J. Nucl. Med. 61 (10) (2020) 1476–1483. Oct.

[168] C. Schuchardt, J. Zhang, H.R. Kulkarni, X. Chen, D. Mueller, R.P. Baum, Prostate-specific membrane antigen radioligand therapy using 177Lu-PSMA I&T and 177Lu-PSMA-617 in patients with metastatic castration-resistant prostate cancer: comparison of safety, biodistribution and dosimetry, J. Nucl. Med. (2021), https://doi.org/10.2967/jnumed.121.262713. Dec 9.

[169] S. Okamoto, A. Thieme, J. Allmann, C. D'Alessandria, T. Maurer, M. Retz, et al., Radiation dosimetry for 177Lu-PSMA I&T in metastatic castration-resistant prostate cancer: absorbed dose in normal organs and tumor lesions, J. Nucl. Med. 58 (3) (2017) 445–450. Mar.

[170] M.J. Zacherl, F.J. Gildehaus, L. Mittlmeier, G. Böning, A. Gosewisch, V. Wenter, et al., First clinical results for PSMA-targeted α-therapy using 225Ac-PSMA-I&T in advanced-mCRPC patients, J. Nucl. Med. 62 (5) (2021) 669–674. May 10.

[171] H. Ilhan, A. Gosewisch, G. Böning, F. Völter, M. Zacherl, M. Unterrainer, et al., Response to 225Ac-PSMA-I&T after failure of long-term 177Lu-PSMA RLT in mCRPC, Eur. J. Nucl. Med. Mol. Imaging 48 (4) (2021) 1262–1263. Apr.

[172] K.P. Maresca, S.M. Hillier, F.J. Femia, D. Keith, C. Barone, J.L. Joyal, et al., A series of halogenated heterodimeric inhibitors of prostate specific membrane antigen (PSMA) as radiolabeled probes for targeting prostate cancer, J. Med. Chem. 52 (2) (2009) 347–357. Jan 22.

[173] S.M. Hillier, K.P. Maresca, F.J. Femia, J.C. Marquis, C.A. Foss, N. Nguyen, et al., Preclinical evaluation of novel glutamate-urea-lysine analogues that target prostate-specific membrane antigen as molecular imaging pharmaceuticals for prostate cancer, Cancer Res. 69 (17) (2009) 6932–6940. Sep 1.

[174] Y. Chen, C.A. Foss, Y. Byun, S. Nimmagadda, M. Pullambhatla, J.J. Fox, et al., Radiohalogenated prostate-specific membrane antigen (PSMA)-based ureas as imaging agents for prostate cancer, J. Med. Chem. 51 (24) (2008) 7933–7943. Dec 25.

[175] A.P. Kiess, I. Minn, Y. Chen, R. Hobbs, G. Sgouros, R.C. Mease, et al., Auger Radiopharmaceutical Therapy Targeting Prostate-Specific Membrane Antigen, J. Nucl. Med. 56 (9) (2015) 1401–1407. Sep.

[176] A.P. Kiess, I. Minn, G. Vaidyanathan, R.F. Hobbs, A. Josefsson, C. Shen, et al., (2S)-2-(3-(1-Carboxy-5-(4-211At-Astatobenzamido)Pentyl)Ureido)-pentanedioic acid for PSMA-targeted α-particle radiopharmaceutical therapy, J. Nucl. Med. 57 (10) (2016) 1569–1575. Oct.

[177] G. Vaidyanathan, R.C. Mease, I. Minn, J. Choi, Y. Chen, H. Shallal, et al., Synthesis and preliminary evaluation of 211At-labeled inhibitors of prostate-specific membrane antigen for targeted alpha particle therapy of prostate cancer, Nucl. Med. Biol. 94-95 (2021) 67–80. Apr.

[178] J. Kelly, A. Amor-Coarasa, S. Ponnala, A. Nikolopoulou, C. Williams, D. Schlyer, et al., Trifunctional PSMA-targeting constructs for prostate cancer with unprecedented localization to LNCaP tumors, Eur. J. Nucl. Med. Mol. Imaging 45 (11) (2018) 1841–1851. Oct.

[179] C.E. Dumelin, S. Trüssel, F. Buller, E. Trachsel, F. Bootz, Y. Zhang, et al., A portable albumin binder from a DNA-encoded chemical library, Angew. Chem. Int. Ed Engl. 47 (17) (2008) 3196–3201.

[180] J.M. Kelly, A. Amor-Coarasa, S. Ponnala, A. Nikolopoulou, C. Williams, S. G. DiMagno, et al., Albumin-binding PSMA Ligands: implications for expanding the therapeutic window, J. Nucl. Med. 60 (5) (2019) 656–663. May.

[181] S. Vallabhajosula, I. Kuji, K.A. Hamacher, S. Konishi, L. Kostakoglu, P.A. Kothari, et al., Pharmacokinetics and biodistribution of 111In- and 177Lu-labeled J591 antibody specific for prostate-specific membrane antigen: prediction of 90Y-J591 radiation dosimetry based on 111In or 177Lu? J. Nucl. Med. 46 (4) (2005) 634–641. Apr.

[182] J.M. Kelly, A. Amor-Coarasa, S. Ponnala, A. Nikolopoulou, C. Williams, N. A. Thiele, et al., A single dose of 225Ac-RPS-074 induces a complete tumor response in an LNCaP xenograft model, J. Nucl. Med. 60 (5) (2019) 649–655. May.

[183] N.A. Thiele, V. Brown, J.M. Kelly, A. Amor-Coarasa, U. Jermilova, S. N. MacMillan, et al., An eighteen-membered macrocyclic ligand for actinium-225 targeted alpha therapy, Angew. Chem. Int. Ed Engl. 56 (46) (2017) 14712–14717. Nov 13.

[184] M. Benešová, C.A. Umbricht, R. Schibli, C. Müller, Albumin-binding PSMA ligands: optimization of the tissue distribution profile, Mol. Pharm. 15 (3) (2018) 934–946. Mar 5.

[185] H.T. Kuo, H. Merkens, Z. Zhang, C.F. Uribe, J. Lau, C. Zhang, et al., Enhancing treatment efficacy of 177Lu-PSMA-617 with the conjugation of an albumin-binding motif: preclinical dosimetry and endoradiotherapy studies, Mol. Pharm. 15 (11) (2018) 5183–5191. Nov 5.

[186] H.T. Kuo, K.S. Lin, Z. Zhang, C.F. Uribe, H. Merkens, C. Zhang, et al., 177Lu-labeled albumin-binder-conjugated PSMA-targeting agents with extremely high tumor uptake and enhanced tumor-to-kidney absorbed dose ratio, J. Nucl. Med. 62 (4) (2021) 521–527. Apr.

[187] L.M. Deberle, V.J. Tschan, F. Borgna, F. Sozzi-Guo, P. Bernhardt, R. Schibli, et al., Albumin-binding PSMA radioligands: impact of minimal structural changes on the tissue distribution profile, Molecules 25 (11) (2020). May 29.

[188] L.M. Deberle, M. Benešová, C.A. Umbricht, F. Borgna, M. Büchler, K. Zhernosekov, et al., Development of a new class of PSMA radioligands comprising ibuprofen as an albumin-binding entity, Theranostics 10 (4) (2020) 1678–1693. Jan 1.

[189] Z. Wang, R. Tian, G. Niu, Y. Ma, L. Lang, L.P. Szajek, et al., Single low-dose injection of evans blue modified PSMA-617 radioligand therapy eliminates prostate-specific membrane antigen positive tumors, Bioconjug. Chem. 29 (9) (2018) 3213–3221. Sep 19.

[190] J. Zang, X. Fan, H. Wang, Q. Liu, J. Wang, H. Li, et al., First-in-human study of 177Lu-EB-PSMA-617 in patients with metastatic castration-resistant prostate cancer, Eur. J. Nucl. Med. Mol. Imaging 46 (1) (2019) 148–158. Jan.

[191] J. Zang, Q. Liu, H. Sui, R. Wang, O. Jacobson, X. Fan, et al., 177Lu-EB-PSMA radioligand therapy with escalating doses in patients with metastatic castration-resistant prostate cancer, J. Nucl. Med. 61 (12) (2020) 1772–1778. Dec.

[192] V. Kramer, R. Fernández, W. Lehnert, L.D. Jiménez-Franco, C. Soza-Ried, E. Eppard, et al., Biodistribution and dosimetry of a single dose of albumin-binding ligand [177Lu]Lu-PSMA-ALB-56 in patients with mCRPC, Eur. J. Nucl. Med. Mol. Imaging 48 (3) (2021) 893–903. Mar.

[193] Z. Wang, O. Jacobson, R. Tian, R.C. Mease, D.O. Kiesewetter, G. Niu, et al., Radioligand therapy of prostate cancer with a long-lasting prostate-specific membrane antigen targeting agent 90Y-DOTA-EB-MCG, Bioconjug. Chem. 29 (7) (2018) 2309–2315. Jul 18.

[194] C.J. Choy, X. Ling, J.J. Geruntho, S.K. Beyer, J.D. Latoche, B. Langton-Webster, et al., 177Lu-labeled phosphoramidate-based PSMA inhibitors: the effect of an albumin binder on biodistribution and therapeutic efficacy in prostate tumor-bearing mice, Theranostics 7 (7) (2017) 1928–1939. Apr 27.
[195] X. Ling, J.D. Latoche, C.J. Choy, B.F. Kurland, C.M. Laymon, Y. Wu, et al., Preclinical dosimetry, imaging, and targeted radionuclide therapy studies of Lu-177-labeled albumin-binding, PSMA-targeted CTT1403, Mol. Imaging Biol. 22 (2) (2020) 274–284. Apr.
[196] P.F. Jackson, D.C. Cole, B.S. Slusher, S.L. Stetz, L.E. Ross, B.A. Donzanti, et al., Design, synthesis, and biological activity of a potent inhibitor of the neuropeptidase N-acetylated alpha-linked acidic dipeptidase, J. Med. Chem. 39 (2) (1996) 619–622. Jan 19.
[197] T.M. Kalidindi, S.G. Lee, K. Jou, G. Chakraborty, M. Skafida, S.T. Tagawa, et al., A simple strategy to reduce the salivary gland and kidney uptake of PSMA-targeting small molecule radiopharmaceuticals, Eur. J. Nucl. Med. Mol. Imaging 48 (8) (2021) 2642–2651. Jul.
[198] M. Eder, M. Schäfer, U. Bauder-Wüst, W.E. Hull, C. Wängler, W. Mier, et al., 68Ga-complex lipophilicity and the targeting property of a urea-based PSMA inhibitor for PET imaging, Bioconjug. Chem. 23 (4) (2012) 688–697. Apr 18.
[199] M. Eder, O. Neels, M. Müller, U. Bauder-Wüst, Y. Remde, M. Schäfer, et al., Novel preclinical and radiopharmaceutical aspects of [68Ga]Ga-PSMA-HBED-CC: a new PET tracer for imaging of prostate cancer, Pharmaceuticals 7 (7) (2014) 779–796. BaselJun 30.
[200] S.Y. Cho, K.L. Gage, R.C. Mease, S. Senthamizhchelvan, D.P. Holt, A. Jeffrey-Kwanisai, et al., Biodistribution, tumor detection, and radiation dosimetry of 18F-DCFBC, a low-molecular-weight inhibitor of prostate-specific membrane antigen, in patients with metastatic prostate cancer, J. Nucl. Med. 53 (12) (2012) 1883–1891. Dec.
[201] S.R. Banerjee, V. Kumar, A. Lisok, J. Chen, I. Minn, M. Brummet, et al., 177Lu-labeled low-molecular-weight agents for PSMA-targeted radiopharmaceutical therapy, Eur. J. Nucl. Med. Mol. Imaging 46 (12) (2019) 2545–2557. Nov.
[202] B. Grubmüller, R.P. Baum, E. Capasso, A. Singh, Y. Ahmadi, P. Knoll, et al., 64Cu-PSMA-617 PET/CT imaging of prostate adenocarcinoma: first in-human studies, Cancer Biother. Radiopharm. 31 (8) (2016) 277–286. Oct 7.
[203] S. Hoberück, G. Wunderlich, E. Michler, T. Hölscher, M. Walther, D. Seppelt, et al., Dual-time-point 64 Cu-PSMA-617-PET/CT in patients suffering from prostate cancer, J. Label. Compd. Radiopharm. 62 (8) (2019) 523–532. Jun 30.
[204] J.R. Nedrow, J.D. Latoche, K.E. Day, J. Modi, T. Ganguly, D. Zeng, et al., Targeting PSMA with a Cu-64 labeled phosphoramidate inhibitor for PET/CT imaging of variant PSMA-expressing xenografts in mouse models of prostate cancer, Mol. Imaging Biol. 18 (3) (2016) 402–410.
[205] S.R. Banerjee, M. Pullambhatla, C.A. Foss, S. Nimmagadda, R. Ferdani, C. J. Anderson, et al., ^{64}Cu-labeled inhibitors of prostate-specific membrane antigen for PET imaging of prostate cancer, J. Med. Chem. 57 (6) (2014) 2657–2669. Mar 27.
[206] C.A. Umbricht, M. Benešová, R. Hasler, R. Schibli, N.P. van der Meulen, C. Müller, Design and preclinical evaluation of an albumin-binding PSMA ligand for 64Cu-based PET imaging, Mol. Pharm. 15 (12) (2018) 5556–5564. Dec 3.
[207] J.M. Kelly, S. Ponnala, A. Amor-Coarasa, N.A. Zia, A. Nikolopoulou, C. Williams, et al., Preclinical evaluation of a high-affinity sarcophagine-containing PSMA ligand for 64Cu/67Cu-based theranostics in prostate cancer, Mol. Pharm. 17 (6) (2020) 1954–1962. Jun 1.
[208] N.A. Zia, C. Cullinane, J.K. Van Zuylekom, K. Waldeck, L.E. McInnes, G. Buncic, et al., A bivalent inhibitor of prostate specific membrane antigen radiolabeled with copper-64 with high tumor uptake and retention, Angew. Chem. Int. Ed Engl. 58 (42) (2019) 14991–14994. Oct 14.
[209] Rodney J Hicks, Price Jackson, Grace Kong, Robert E Ware, Michael S Hofman, David A Pattison, et al., ^{64}Cu-SARTATE PET Imaging of Patients with Neuroendocrine Tumors Demonstrates High Tumor Uptake and Retention, Potentially Allowing Prospective Dosimetry for Peptide Receptor Radionuclide Therapy, J Nucl Med 60 (6) (2019) 777–785.
[210] L.E. McInnes, C. Cullinane, P.D. Roselt, S. Jackson, B.J. Blyth, E.M. van Dam, et al., Therapeutic efficacy of a bivalent inhibitor of prostate-specific membrane antigen labeled with 67Cu, J. Nucl. Med. 62 (6) (2021) 829–832. Jun 1.
[211] K.A. Domnanich, C. Müller, M. Benešová, R. Dressler, S. Haller, U. Köster, et al., 47Sc as useful β–emitter for the radiotheragnostic paradigm: a comparative study of feasible production routes, EJNMMI Radiopharm. Chem. 2 (1) (2017) 5. Jun 2.
[212] R. Walczak, S. Krajewski, K. Szkliniarz, M. Sitarz, K. Abbas, J. Choiński, et al., Cyclotron production of (43)*Sc* for PET imaging, EJNMMI Phys. 2 (1) (2015) 33. Dec 4.
[213] E. Eppard, A. de la Fuente, M. Benešová, A. Khawar, R.A. Bundschuh, F. C. Gärtner, et al., Clinical translation and first in-human use of [44Sc]*Sc*-PSMA-617 for PET imaging of metastasized castrate-resistant prostate cancer, Theranostics 7 (18) (2017) 4359–4369. Sep 26.
[214] C.A. Umbricht, M. Benešová, R.M. Schmid, A. Türler, R. Schibli, N.P. van der Meulen, et al., 44Sc-PSMA-617 for radiotheragnostics in tandem with 177Lu-PSMA-617-preclinical investigations in comparison with 68Ga-PSMA-11 and 68Ga-PSMA-617, EJNMMI Res. 7 (1) (2017) 9. Dec.
[215] B.A. Vaughn, A.J. Koller, Z. Chen, S.H. Ahn, C.S. Loveless, S.J. Cingoranelli, et al., Homologous structural, chemical, and biological behavior of sc and lu complexes of the picaga bifunctional chelator: toward development of matched theranostic pairs for radiopharmaceutical applications, Bioconjug. Chem. 32 (7) (2021) 1232–1241. Jul 21.
[216] B.A. Vaughn, C.S. Loveless, S.J. Cingoranelli, D. Schlyer, S.E. Lapi, E. Boros, Evaluation of 177Lu and 47Sc picaga-linked, prostate-specific membrane antigen-targeting constructs for their radiotherapeutic efficacy and dosimetry, Mol. Pharm. 18 (12) (2021) 4511–4519. Dec 6.
[217] J.P. Sinnes, U. Bauder-Wüst, M. Schäfer, E.S. Moon, K. Kopka, F. Rösch, 68Ga, 44Sc and 177Lu-labeled AAZTA5-PSMA-617: synthesis, radiolabeling, stability and cell binding compared to DOTA-PSMA-617 analogues, EJNMMI Radiopharm. Chem. 5 (1) (2020) 28. Nov 26.
[218] C. Müller, C.A. Umbricht, N. Gracheva, V.J. Tschan, G. Pellegrini, P. Bernhardt, et al., Terbium-161 for PSMA-targeted radionuclide therapy of prostate cancer, Eur. J. Nucl. Med. Mol. Imaging 46 (9) (2019) 1919–1930. Aug.
[219] C.A. Umbricht, U. Köster, P. Bernhardt, N. Gracheva, K. Johnston, R. Schibli, et al., Alpha-PET for prostate cancer: preclinical investigation using 149Tb-PSMA-617, Sci. Rep. 9 (1) (2019) 17800. Nov 28.
[220] S.R. Banerjee, I. Minn, V. Kumar, A. Josefsson, A. Lisok, M. Brummet, et al., Preclinical evaluation of 203/212Pb-labeled low-molecular-weight compounds for targeted radiopharmaceutical therapy of prostate cancer, J. Nucl. Med. 61 (1) (2020) 80–88. Jan.
[221] V.Y. Stenberg, R.H. Larsen, L.W Ma, Q. Peng, P. Juzenas, Ø.S. Bruland, et al., Evaluation of the PSMA-binding ligand 212Pb-NG001 in multicellular tumour spheroid and mouse models of prostate cancer, Int. J. Mol. Sci. 22 (9) (2021). May 1.
[222] S. Hammer, U.B. Hagemann, S. Zitzmann-Kolbe, A. Larsen, C. Ellingsen, S. Geraudie, et al., Preclinical efficacy of a PSMA-targeted thorium-227 conjugate (PSMA-TTC), a targeted alpha therapy for prostate cancer, Clin. Cancer Res. 26 (8) (2020) 1985–1996. Apr 15.
[223] N.A. Thiele, J.J. Woods, J.J. Wilson, Implementing f-block metal ions in medicine: tuning the size selectivity of expanded macrocycles, Inorg. Chem. 58 (16) (2019) 10483–10500. Aug 19.
[224] A. Morgenstern, L.M. Lilley, B.W. Stein, S.A. Kozimor, E.R. Batista, P. Yang, Computer-assisted design of macrocyclic chelators for actinium-225 radiotherapeutics, Inorg. Chem. 60 (2) (2021) 623–632. Jan 18.
[225] H. Yang, C. Zhang, Z. Yuan, C. Rodriguez-Rodriguez, A. Robertson, V. Radchenko, et al., Synthesis and evaluation of a macrocyclic actinium-225 chelator, quality control and *in vivo* evaluation of 225 Ac-crown-αMSH peptide, Chem. Eur. J. 26 (50) (2020) 11435–11440. Sep 4.
[226] A. Hu, V. Brown, S.N. MacMillan, V. Radchenko, H. Yang, L. Wharton, et al., Chelating the alpha therapy radionuclides $225Ac^{3+}$ and $213Bi^{3+}$ with 18-membered macrocyclic ligands macrodipa and Py-macrodipa, Inorg. Chem. 61 (2) (2022) 801–806. Jan 17.
[227] F. Reissig, D. Bauer, K. Zarschler, Z. Novy, K. Bendova, M.-.C. Ludik, et al., Towards targeted alpha therapy with actinium-225: chelators for mild condition radiolabeling and targeting PSMA-a proof of concept study, Cancers 13 (8) (2021). BaselApr 20.
[228] M.G. Ferrier, Y. Li, M.K. Chyan, R. Wong, L. Li, S. Spreckelmeyer, et al., Thorium chelators for targeted alpha therapy: rapid chelation of thorium-226, J. Label. Compd. Radiopharm. 63 (12) (2020) 502–516. Oct.
[229] G.J.P. Deblonde, T.D. Lohrey, C.H. Booth, K.P. Carter, B.F. Parker, Å. Larsen, et al., Solution thermodynamics and kinetics of metal complexation with a hydroxypyridinone chelator designed for thorium-227 targeted alpha therapy, Inorg. Chem. 57 (22) (2018) 14337–14346. Nov 19.
[230] B.L. McNeil, A.K.H. Robertson, W. Fu, H. Yang, C. Hoehr, C.F. Ramogida, et al., Production, purification, and radiolabeling of the 203Pb/212Pb theranostic pair, EJNMMI Radiopharm. Chem. 6 (1) (2021) 6. Feb 1.
[231] J. Ma, L. Li, T. Liao, W. Gong, C. Zhang, Efficacy and safety of 225Ac-PSMA-617-targeted alpha therapy in metastatic castration-resistant prostate cancer: a systematic review and meta-analysis, Front. Oncol. 12 (2022), 796657. Feb 3.
[232] S. Satapathy, A. Sood, C.K. Das, B.R. Mittal, Evolving role of 225Ac-PSMA radioligand therapy in metastatic castration-resistant prostate cancer-a systematic review and meta-analysis, Prostate Cancer Prostatic Dis. 24 (3) (2021) 880–890. Sep.
[233] T. Langbein, G. Chaussé, R.P. Baum, Salivary gland toxicity of PSMA radioligand therapy: relevance and preventive strategies, J. Nucl. Med. 59 (8) (2018) 1172–1173. Aug.
[234] B. Yilmaz, S. Nisli, N. Ergul, R.U. Gursu, O. Acikgoz, T.F. Çermik, Effect of external cooling on 177Lu-PSMA uptake by the parotid glands, J. Nucl. Med. 60 (10) (2019) 1388–1393. Oct.
[235] H. Rathke, C. Kratochwil, R. Hohenberger, F.L. Giesel, F. Bruchertseifer, P. Flechsig, et al., Initial clinical experience performing sialendoscopy for salivary gland protection in patients undergoing 225Ac-PSMA-617 RLT, Eur. J. Nucl. Med. Mol. Imaging 46 (1) (2019) 139–147. Jan.
[236] R.P. Baum, T. Langbein, A. Singh, M. Shahinfar, C. Schuchardt, G.F. Volk, et al., Injection of botulinum toxin for preventing salivary gland toxicity after PSMA radioligand therapy: an empirical proof of a promising concept, Nucl. Med. Mol. Imaging 52 (1) (2018) 80–81. Feb.
[237] J. Mueller, T. Langbein, A. Mishra, R.P. Baum, Safety of high-dose botulinum toxin injections for parotid and submandibular gland radioprotection, Toxins (Basel) 14 (1) (2022) 64. BaselJan 17.
[238] E. Rousseau, J. Lau, H.T. Kuo, Z. Zhang, H. Merkens, N. Hundal-Jabal, et al., Monosodium glutamate reduces 68Ga-PSMA-11 uptake in salivary glands and kidneys in a preclinical prostate cancer model, J. Nucl. Med. 59 (12) (2018) 1865–1868. Dec.
[239] A. Sarnelli, M.L. Belli, V. Di Iorio, E. Mezzenga, M. Celli, S. Severi, et al., Dosimetry of 177Lu-PSMA-617 after mannitol infusion and glutamate tablet administration: preliminary results of EUDRACT/RSO 2016-002732-32 IRST protocol, Molecules 24 (3) (2019) 624. Feb 11.
[240] G. Paganelli, A. Sarnelli, S. Severi, M. Sansovini, M.L. Belli, M. Monti, et al., Dosimetry and safety of 177Lu PSMA-617 along with polyglutamate parotid gland

protector: preliminary results in metastatic castration-resistant prostate cancer patients, Eur. J. Nucl. Med. Mol. Imaging 47 (13) (2020) 3008–3017. Dec.
[241] D.G. Burrin, B. Stoll, Metabolic fate and function of dietary glutamate in the gut, Am. J. Clin. Nutr. 90 (3) (2009) 850S–856S. Sep.
[242] A.B. Tucker, S.D. Stocker, Hypernatremia-induced vasopressin secretion is not altered in TRPV1-/- rats, Am. J. Physiol. Regul. Integr. Comp. Physiol. 311 (3) (2016) R451–R456. Sep 1.
[243] J.A. Ship, D.J. Fischer, The relationship between dehydration and parotid salivary gland function in young and older healthy adults, J. Gerontol. A Biol. Sci. Med. Sci. 52 (5) (1997) M310–M319. Sep.
[244] G. Iorgulescu, Saliva between normal and pathological. Important factors in determining systemic and oral health, J. Med. Life 2 (3) (2009) 303–307. Sep.
[245] A.M.L. Pedersen, C.E. Sørensen, G.B. Proctor, G.H. Carpenter, J. Ekström, Salivary secretion in health and disease, J. Oral Rehabil. 45 (9) (2018) 730–746. Sep.
[246] S. Mahernia, A. Amanlou, G. Kiaee, M. Amanlou, Determination of hydrogen cyanide concentration in mainstream smoke of tobacco products by polarography, J. Environ. Health Sci. Eng. 13 (1) (2015) 57. Jul 29.
[247] M.J. Gardner, T.L. McCarthy, W.J. Jusko, Relationship of serum thiocyanate concentrations to smoking characteristics, J. Toxicol. Environ. Health 14 (2–3) (1984) 393–406.
[248] E.L. Thomas, M.M. Jefferson, R.E. Joyner, G.S. Cook, C.C. King, Leukocyte myeloperoxidase and salivary lactoperoxidase: identification and quantitation in human mixed saliva, J. Dent. Res. 73 (2) (1994) 544–555. Feb.
[249] M.T. Ashby, Inorganic chemistry of defensive peroxidases in the human oral cavity, J. Dent. Res. 87 (10) (2008) 900–914. Oct.
[250] M.J. Davies, Myeloperoxidase: mechanisms, reactions and inhibition as a therapeutic strategy in inflammatory diseases, Pharmacol. Ther. 218 (2021), 107685. Feb.
[251] D.I. Pattison, M.J. Davies, C.L. Hawkins, Reactions and reactivity of myeloperoxidase-derived oxidants: differential biological effects of hypochlorous and hypothiocyanous acids, Free Radic. Res. 46 (8) (2012) 975–995. Aug.
[252] O.P. Foss, P.G. Lund-Larsen, Serum thiocyanate and smoking: interpretation of serum thiocyanate levels observed in a large health study, Scand. J. Clin. Lab. Invest. 46 (3) (1986) 245–251. May.
[253] J. Flieger, J. Kawka, M. Tatarczak-Michalewska, Levels of the thiocyanate in the saliva of tobacco smokers in comparison to e-cigarette smokers and nonsmokers measured by HPLC on a phosphatidylcholine column, Molecules 24 (20) (2019) 3790. Oct 21.
[254] R. Maas, V. Xanthakis, T. Göen, J. Müller, E. Schwedhelm, R.H. Böger, et al., Plasma nitrate and incidence of cardiovascular disease and all-cause mortality in the community: the framingham offspring study, J. Am. Heart Assoc. 6 (11) (2017). Nov 18.
[255] A.F. Badawi, G. Hosny, M. el-Hadary, M.H. Mostafa, Salivary nitrate, nitrite and nitrate reductase activity in relation to risk of oral cancer in Egypt, Dis. Markers 14 (2) (1998) 91–97. Oct.
[256] S.A. Omar, A.J. Webb, J.O. Lundberg, E. Weitzberg, Therapeutic effects of inorganic nitrate and nitrite in cardiovascular and metabolic diseases, J. Intern. Med. 279 (4) (2016) 315–336. Apr.
[257] X. Feng, Z. Wu, J. Xu, Y. Xu, B. Zhao, B. Pang, et al., Dietary nitrate supplementation prevents radiotherapy-induced xerostomia, Elife 10 (2021). Sep 28.
[258] L. Li, H. Wang, L. Hu, X. Wu, B. Zhao, Z. Fan, et al., Age associated decrease of sialin in salivary glands, Biotech. Histochem. 93 (7) (2018) 505–511. May 23.
[259] L. Dubois, N. Pietrancosta, A. Cabaye, I. Fanget, C. Debacker, P.-.A. Gilormini, et al., Amino acids bearing aromatic or heteroaromatic substituents as a new class of ligands for the lysosomal sialic acid transporter sialin, J. Med. Chem. 63 (15) (2020) 8231–8249. Aug 13.
[260] J. Lodder-Gadaczek, V. Gieselmann, M. Eckhardt, Vesicular uptake of N-acetylaspartylglutamate is catalysed by sialin (SLC17A5), Biochem. J. 454 (1) (2013) 31–38. Aug 15.
[261] L. Qin, X. Liu, Q. Sun, Z. Fan, D. Xia, G. Ding, et al., Sialin (SLC17A5) functions as a nitrate transporter in the plasma membrane, Proc. Natl. Acad. Sci. USA 109 (33) (2012) 13434–13439. Aug 14.
[262] S.S. Chang, V.E. Reuter, W.D. Heston, N.H. Bander, L.S. Grauer, P.B. Gaudin, Five different anti-prostate-specific membrane antigen (PSMA) antibodies confirm PSMA expression in tumor-associated neovasculature, Cancer Res. 59 (13) (1999) 3192–3198. Jul 1.
[263] M.R. Naunheim, H.W. Lin, W.C. Faquin, D.T. Lin, Intercalated duct lesion of the parotid, Head Neck Pathol. 6 (3) (2012) 373–376. Sep.
[264] Y. Mok, Y.H. Pang, M. Teh, F. Petersson, Hybrid intercalated duct lesion of the parotid: diagnostic challenges of a recently described entity with fine needle aspiration findings, Head Neck Pathol. 10 (2) (2016) 269–274. Jun.
[265] N. Pietrancosta, C. Anne, H. Prescher, R. Ruivo, C. Sagné, C. Debacker, et al., Successful prediction of substrate-binding pocket in SLC17 transporter sialin, J. Biol. Chem. 287 (14) (2012) 11489–11497. Mar 30.
[266] Y. Xu, S. Szép, Z. Lu, The antioxidant role of thiocyanate in the pathogenesis of cystic fibrosis and other inflammation-related diseases, Proc. Natl. Acad. Sci. USA 106 (48) (2009) 20515–20519. Dec 1.
[267] J.D. Chandler, B.J. Day, Thiocyanate: a potentially useful therapeutic agent with host defense and antioxidant properties, Biochem. Pharmacol. 84 (11) (2012) 1381–1387. Dec 1.
[268] C. Guo, M.J. Davies, C.L. Hawkins, Role of thiocyanate in the modulation of myeloperoxidase-derived oxidant induced damage to macrophages, Redox. Biol. 36 (2020), 101666. Sep.
[269] P. Aggarwal, K.A. Hutcheson, R. Yu, J. Wang, C.D. Fuller, A.S. Garden, et al., Genetic susceptibility to patient-reported xerostomia among long-term oropharyngeal cancer survivors, Sci. Rep. 12 (1) (2022) 6662. Apr 22.
[270] E.H.N. Pow, Z. Chen, D.L.W. Kwong, O.L.T Lam, Salivary anionic changes after radiotherapy for nasopharyngeal carcinoma: a 1-year prospective study, PLoS One 11 (3) (2016), e0152817. Mar 31.
[271] J. Li, Z. Shan, G. Ou, X. Liu, C. Zhang, B.J. Baum, et al., Structural and functional characteristics of irradiation damage to parotid glands in the miniature pig, Int. J. Radiat. Oncol. Biol. Phys. 62 (5) (2005) 1510–1516. Aug 1.
[272] S.L. Wang, J. Li, X.Z. Zhu, K. Sun, X.Y. Liu, Y.G. Zhang, Sialographic characterization of the normal parotid gland of the miniature pig, Dentomaxillofac. Radiol. 27 (3) (1998) 178–181. May.
[273] P. Backhaus, B. Noto, N. Avramovic, L.S. Grubert, S. Huss, M. Bögemann, et al., Targeting PSMA by radioligands in non-prostate disease-current status and future perspectives, Eur. J. Nucl. Med. Mol. Imaging 45 (5) (2018) 860–877. May.